IJAAR PUBLISHING®

Engineering Research Journal | ISSN: 2782-8212
Vol. 4, Issue 9 (September, 2024) | www.ijaar.org/erj

Enhancing the corrosion inhibition performance of *Ocimum gratissimum* crude extract in 3.5 % NaCl through synergism with Zinc Sulphate Heptahydrate: Experimental and Computational Studies.

Columbus L. O.[1], Njoku D. I. [2], Chidiebere M. A. [1,3]*, Nwanonenyi S. C. [1,4], Onyeachu B. I. [1,5], Benedict C.[6], Oguzie E. E. [1]

[1]Africa Centre of Excellence in Future Energies and Electrochemical Systems, Federal University of Technology, PMB 1526, Owerri, Nigeria
[2]Institute of Metal Research, Chinese Academy of Sciences, 62 Wencui Road, Shenyang, 110016, China
[3]Department of Science Laboratory Technology, Federal University of Technology, Owerri, PMB 1526, Owerri, Nigeria
[4]Department of Polymer Science and Engineering, Federal University of Technology, Owerri, PMB 1526, Owerri, Nigeria
[5]Department of Industrial Chemistry, Faculty of Science, Edo State University, Uzairue Iyamho, Nigeria
[6]Department of Chemical Engineering, Faculty of Engineering, Federal Polytechnic Nekede, Owerri, Nigeria.
**** Corresponding author's E-mail address: columbuslotanna123@gmail.com or ohia.columbus@acefuels-futo.org***

Abstract

This study investigates the corrosion inhibition action of Ocimum gratissimum (OG) biomass extract and the blend with Zinc Sulphate heptahydrate (ZS) on mild steel corrosion in 3.5 Wt. % NaCl environment. Combined gravimetric and advanced characterization techniques including gas chromatography–mass spectrometry (GC-MS) and ultraviolet, visible, near-infrared (UV-VIS-NIR) spectroscopic studies were employed in the investigation. The results of the gravimetric studies revealed a very low inhibition efficiency with maximum value of 21.9% for the biomass at concentration of 0.25 g/L whereas, upon blending with the optimal amounts of ZS, higher inhibition efficiency values reaching 93.1%, was obtained. Unlike in the unblended system, the obtained IE% values for the blends were almost stable even at 120 h of immersion time. The study of the synergistic index of the extract and the additives showed a cooperative interaction. The GC-MS analysis revealed a number of biomass extract constituents that contain hetero-atoms like sulfur, oxygen, and nitrogen, validating their propensity to inhibit the mild steel coupon corrosion in 3.5 wt%. NaCl environment with Methylene Chloride, Thymol and Benzene, 1 methyl-3-(1-methylethyl) as major constituents of the extract. The UV-VIS-NIR studies also showed that the biomass final blends do not loose chromophore at intervals of 24 h, 72 h, 96 h and 120 h, indicating that the active constituents in the final blends do not degrade within the investigation period. Quantum Chemical studies were used to complement experimental and surface probe analysis.

Keywords: Biomass extract; Inhibitor; Blends; Corrosion; Synergism; Density Functional Theory, Atomic Force Microscopy.

Columbus L. O., Njoku D. I., Chidiebere M. A., Nwanonenyi S. C., Onyeachu B. I., Benedict C. & Oguzie E. E. (2024). Enhancing the corrosion inhibition performance of *Ocimum gratissimum* crude extract in 3.5 % NaCl through synergism with Zinc Sulphate Heptahydrate: Experimental and Computational Studies. *Engineering Research Journal, 10*(9), 31-54. DOI: 10.5281/zenodo.13901569

Introduction

Mild steel remains the most often used metallic material, particularly in marine environment, mechanical engineering as well as oil and gas industries. However, a common issue known as corrosion limits the usefulness of metals and their alloys, (Divya *et al*., 2019; Kermani & Morshed, 2003; Papavinasam, 2013). To reduce the rate of electrochemical corrosion, the primary technique is to keep the metal away from materials that are corrosive. The most effective and popularly utilized approach employed to isolate metals surfaces from the corrosive environment is the introduction of corrosion inhibitors, (Anupama *et al.*, 2016). The use of corrosion inhibitors for metals and alloys, Some researchers studying corrosion phenomena are interested in corrosion deterioration restriction, (Rahal et al., 2016; Sanaei et al., 2018). Also, it has been demonstrated that organic molecules, like azole compounds, have beneficial effects on the corrosion protection of steel, aluminum alloys, and copper metallic substrates in acidic conditions. (Ramezanzadeh *et al*., 2017). Aside from media that is acidic, certain steel constructions are exposed to neutral/alkaline/salt water environment, hence the metals exposed to these service environment should have their corrosion mitigated, (Adekanmi & Olowofoyeku, 2020; Amar et al., 2006; Fawzy et al., 2018; Udensi et al., 2021). High-potency inhibitors for metals can be found in organic compounds, including heteroatoms, which are composed of polar groups, conjugated bonds (C-C), and electron-rich atoms like O, N, and S, (Bahlakeh et al., 2017; Njokua et al., 2013). By interacting chemically or physically with the atoms close to the metal surface, they can reduce the reactivity of the metals to corrosion, (Divya *et al*., 2019). The crude extracts of plants contain active species (phytochemicals) that suppresses the corrosion deterioration of metal substance in the acidic media. However, the organic moieties that highly tend to adsorb on the metallic surfaces in acidic media show a low tendency to adsorption on the metallic surface in neutral media like NaCl, (Anupama et al., 2016; Khadija et al., 2018; Mohammed & Al-Fakih, 2017). Recently, some researchers have looked into how inorganic species and organic inhibitors work together to reduce corrosion. (Kaghazchi et al., 2021; Ramezanzadeh et al., 2019a; Tabatabaei majd et al., 2019). The synergistic corrosion retardation effect of Zn^{2+}- Nettle was investigated in a paper by (Bahlakeh et al., 2017), their findings revealed a uniform layer generation on the steel substrate surface exposed to the Zn^{2+} cations and NLE containing NaCl solution. In reality, the formation of an inhibitive coating on the reactive sites of the metal surface that are exposed to corrosive species may be the consequence of the chelation between the Fe^{2+}/Zn^{2+} metal cations and functional groups containing electron-rich elements (such as NH_2 and OH). (Motamedi et al., 2018)have demonstrated the beneficial inhibitory effect of a few additional complexes, including praseodymium nitrate (PrN) and plant extract from Urtica dioica.

Synergistic effect of additives such as zinc ion and natural polymers, zinc ions specifically have been used as inhibitor additives as studied by (Kaghazchi *et al*., 2021; Ramezanzadeh *et al*., 2019a). The zinc ions were either needed in large quantity to achieve metal protection while other studies showed that the zinc ions yielded high inhibition efficiency but decline in protection efficiency over time. This study considered blending of additives that will equally tackle the aforementioned limitations. They additives are needed in little concentration to achieve maximum protection and a long-lasting inhibitor blend for mild steel in neutral media.

Many researchers have investigated the inhibitive performance of many organic molecules and recorded many different challenges including environmental unfriendliness, toxicity to aquatic life and disposal challenges, (Amar et al., 2006; Amiery et al., 2022; Doubi et al., 2020; El-hafez & Badawy, 2013; Fawzy et al., 2018; Loto et al., 2020; Mobin & Aslam, 2018; Pech-Canul & Bartolo-Pérez, 2004; Peng et al., 2018; Ramesh & Rajeswari, 2004; Singh et al., 2015; Verma et al., 2017).

A more saver approach has been the use of inorganic inhibitors which is more environmentally friendly, they are not cost effective, (Aramaki, 2001; Cotting & Vieira, n.d.; Miralrio & Vázquez, 2020; Verma et al., 2017). Also, they perform very poorly in the neutral environment thus, there is a great need for the modification and/or replacement of these compounds to enable better interaction with the environment and enhancement of their inhibition efficiencies.

Employing biomass-derived materials for steel protection against corrosion has been a more reliable and feasible propositions for industrial applications, in contrast, their application in neutral environment recorded proven material protection that lose inhibition effectiveness over time, (Al Otaibi & Hammud, 2021; Alam et al., 2021; Casaletto et al., 2018; G & O, 2017; Haddadi et al., 2019; Hajar et al., 2016; Ikhmal et al., 2019, 2020; Naghi Tehrani et al., 2021; Palaniappan et al., 2020; Rizvi et al., 2020; Shabani-Nooshabadi & Ghandchi, 2015; Udensi et al., 2021). They usually don't perform well in such media thus the need to evaluate their protective capability in synergism with salts and natural polymers that are cheap, available and environmentally friendly. *OG* (African Basil) is a well-known plant (called *Nchanwu*) among the Igbo people of Nigeria in West Africa. The leaf of *OG* are used in medicine and as a spice in the preparation of certain tubers. OG leaf extracts have reportedly shown poor inhibition performance in neutral environment unlike its performance when applied in acidic media. The performance of OG showed a significant decrease in protection efficiency as immersion time

increases showing that the active components of the extract lose their inhibitive strengths as reaction progresses in the electrolyte environment, (Blessing *et al.*, 2017; Eddy *et al.*, 2010; Ikpeseni *et al*., 2021).

The objective of this study is to evaluate the corrosion inhibitor blends of *OG* for mild steel corrosion protection in a salt environment which will include; assessment of the crude extracts' ability to inhibit corrosion in 3.5 wt% NaCl solution, with respect to dosage, exposure time and temperature, evaluation of the synergistic impact of Zn^{2+} ions on biomass extract, characterization of the phyto-constituents of each crude extract and application of computational modeling tools to assess the contribution of Phyto-chemical constituents towards the inhibitory performance of each plant extract.

2 Experimental Procedure

2.1 Materials

Metal steel specimens with the following composition (atom %): C (0.16%), Mn (0.64%), P (0.13%), S (0.11%), and Fe (98.95%) were used as the test specimens. The mild steel sample for weight loss studies were cut into small sizes of 3 x 3 cm with 0.1 cm thickness. These steel samples were polished by the use of polishing paper sizes, submerged in pure ethanol, cleaned with acetone, weighed, then kept in a desiccator until needed to avoid contamination and/or further corrosion before usage. The corrosive media for the study was 3.5 Wt. % NaCl (Sodium chloride). This was prepared using distilled water. Every test was conducted at room temperature in an oxygenated medium.
The OG leaf was plucked from the farm where they naturally grow and was identified by plant scientist from the Department of Crop Science, Federal University of Technology. This was washed with clean water and allowed to dry at room temperature. The dried leaf was grounded into powdered form using electric blender and, a known mass of the plant powders were soaked with absolute ethanol of 96% purity for a duration of 3 days (72 hours) and thereafter filtered thoroughly. The additive used in this study is zinc salt (ZS).

2.2 Characterization of Extract

2.2.1: Gas Chromatography- Mass Analysis (GC-MS) Characterization

10 g of the plant extract sample in 100 ml of ethanol was employed. The sample was filtered and concentrated in a rotary evaporator to about 2 ml.

Measured 2 µL of the 10 g ethanol sample extract was injected into the GC column for analysis. The GC (Agilent 6890N) and MS (5973 MSD) equipped with Restek capillary column (30 m x 0.25 mm; film thickness 1.4 µm) was used. To identify the unknown phytochemical components present in the samples, their individual mass spectral peak values were compared with the database of national Institute of Science and Technology 2014. (Jain *et al.*, 2016), (Kalaichelvi & Dhivya, 2017).

2.2.2: Fourier Transform Infrared Spectroscopy

With the Nicolet-Magna-IR 560 FTIR spectrophotometer, FTIR spectra were captured. The PG powder spectrum and the protective layer that developed on the mild steel surface during a three-hour immersion in the test solution containing OG, ZS, and OG + ZS, inhibitors were analyzed by carefully removing the metal, scrapping out the films, mixing it with KBr, and making the pellet. With FTIR analysis, the range of infrared wavelengths that a substance absorbs was found. In order to do this, samples of the chemical are exposed to infrared light (IR), (Chidiebere *et al.*, 2015).

2.3 Gravimetric (Corrosion) Measurement

Gravimetric experiments were conducted under total immersion condition in 400 ml of test solution (3.5wt% of NaCl) at room temperature. The coupons were weighed and then, immersed in the test solution. All tests were carried out in aerated and stirred solution. Test coupons were retrieved at 24 h intervals progressively for 120 h, washed in water, dried, cleaned with a bristle brush, and then weighed again. A specific time was chosen for the weight loss. Analytical weighing balance with a range of 0.0001g to 210g (FA210) was used. The formulas below were used to determine the weight loss and corrosion rates:

i) The weight loss (W) was determined by:

$$W_{(g)} = W_1 - W_2 \qquad \text{Eqn. 1}$$

Where W_1 is the weight of steel coupon before immersion, W_2 is the weight of steel coupon after immersion.

ii) Corrosion Rate (CR):

$$C.R = \frac{87600\,W}{DAT} \quad \text{Eqn. 2}$$

Where;

C.R = the rate of corrosion in millimeter per year, W = weight loss (mg), D = density of steel sample (g/cm^3), A = area of specimen exposed to corrosion (cm^2), T = time of exposure (h).

iii)The inhibition efficiency (%) was determined with the equation:

$$IE = 1 - \frac{W_1}{W_2} \times 100 \quad \text{Eqn. 3}$$

Where; IE= Inhibition efficiency, W_1= weight loss of metal in the presence of extract and W_2 = weight loss of metal in the absence of extract.

iv) **Degree of surface coverage (θ):**

$$\theta = \left(\frac{I.E}{100}\right) \quad \text{Eqn. 4}$$

Where; I.E= Inhibition Efficiency (%).

v) **Synergism index (SI):**

$$\boldsymbol{SI} = \frac{\mathbf{1}-\boldsymbol{\eta_{ext}}-\boldsymbol{\eta_{add}}+\boldsymbol{\eta_{ext}}\times\boldsymbol{\eta_{add}}}{\mathbf{1}-\boldsymbol{\eta_{ext:add}}} \quad \text{Eqn. 5}$$

Where: η_{ext} represents the efficiency of inhibition by the plant extracts, η_{add} represents efficiency in inhibition of the additives.

2.4 Adsorption studies

The isotherm of adsorption was studied to predict and obtain insights into the interaction between the metal surface and the respective inhibitors. This was calculated using the equation below:

$$\frac{C}{\theta} = \frac{1}{K_{ads}} + C \quad \text{Eqn. 6}$$

With C being the inhibitor concentration in ppm, K_{ads} being the adsorption equilibrium constant and θ being the degree of surface coverage.

2.5 UV–Visible Spectroscopy

The Shimadzu UV-VIS-NIR Spectrophotometer (UV-3600) was used in the analysis of the inhibition solution. This device was used to detect the presence of unsaturated or absence of heteroatoms and functional groups present in the plant leaf solutions over time as well as to monitor the degradation and absorption features of these solutions as the gravimetric analysis goes on, (Vijayakumar *et al.*, 2018). The individual inhibitor solutions prepared were taken in adequate proportion and placed into a cuvette with a reference solution containing absolute ethanol. They were used to run the analysis and the results recorded.

2.6 Computational Studies

The density functional theory (DFT) calculations were carried out with the aid of DMol^3 package. DMol^3 is used to model the electronic structure and energies of molecules and surfaces using density functional *theory* (DFT). Utilizing a Mulliken population analysis, this was accomplished. Vital parameters for example, lowest unoccupied molecular orbital (E_{LUMO}) and highest occupied molecular orbital (E_{HUMO}), and the energy gap ΔE ($E_{LUMO} - E_{HOMO}$), were obtained for the selected active components of the plant extract, polymeric inhibitors and organic molecules so as to infer its activity toward the Fe surface. More of the theoretical parameters to be calculated using computational studies include:

Ionization Energy (I) = $-E_{HOMO}$

Electron affinity (A) = $-E_{LUMO}$

Electron charge transfer, (ΔN) =

$$\Delta N = \frac{\chi_m - \chi_i}{2(\eta_m + \eta_i)} \quad \text{Eqn. 7}$$

Where χ_m = the metal's total electronegativity, χ_i= denote the inhibitor molecules' total electronegativity, η_m = denote metals total hardness, η_i = denote the inhibitor's total hardness. χ and η are related to A and I as follow:

$$\chi = \frac{I+A}{2} \quad \text{Eqn. 8}$$

$$\eta = \frac{I+A}{2} \quad \text{Eqn. 9}$$

Additionally, we used Materials Studio software to run molecular dynamics (MD) simulations inside a simulation box with periodic boundary conditions in order to calculate the adsorption energy of the molecules under study onto the Fe (110) surface. First, the iron crystal was imported and cleaved along the (110) plane using a slab of five. Next, the energy of the Fe (110) surface was reduced using the smart minimizer technique, which relaxed it. Finally, the Fe (110) surface was expanded to a (12 x 12) supercell to provide a larger surface area for the organic components' interaction. The adsorption energy between the inhibitor structures and Fe (110) was estimated by calculating the interaction energies using the Equation:

$$E_{(adsorption)} = E_{total} - (E_{surface} + E_{inhibitor}) \quad \text{Eqn. 10}$$

Where

E_{total} denotes the total energy of the system, $E_{surface}$ represents the total energy of Fe (110) surface and $E_{inhibitor}$ signifies the total energy of inhibitor.

3 Results and Discussion

3.1 Gravimetric measurements

The extract from OG and ZS were used to study the corrosion protection of mild steel in 3.5 wt% NaCl environment via gravimetric measurement technique. The corresponding gravimetric results obtained are presented in Figures 1- 3.

3.1.1 ZS and OG Results

The gravimetric evaluation of inhibitory performance of OG and ZS in 3.5 wt.% NaCl are presented in Figure 1. As can be seen in Figure 1b, the ZS exhibited a low inhibition efficiency ranging from 37.8% at 0.05 M for both 24 h and 48 h to 18% at 120 h for 0.001 M concentration. The result reveals that there was desorption of the active components of this inhibitor rather than adsorption on the metal surface over time.

Considering OG results, at 24 h immersion time, the inhibition efficiency is in the order: 21.3 > 20.4 > 18.5 > 15.2% for 1.0 g/L, 0.1 g/L, 0.25 g/L and 0.5 g/L respectively. The inhibition efficiency is found to be decreasing as duration of exposure increases as much as 120 h. There was a clear trend observed showing that the efficiency in the inhibition's decrease is not static, as it decreases within 48 h, 72 h and there was also, a slight rise thereafter except for 0.25 g/L concentration that is on the decrease till 120 h. The overall performance of the protection efficiency of this extract can be likened to the study carried out by (Sangeetha *et al*., 2012), where the extract of banana peel was used as a corrosion inhibitor in NaCl environment. The inhibition efficiency of the system was high but recorded a significant decrease over time up to 7 days. The maximum corrosion rate (mmpy) for this extract was recorded to be 0.53 mmpy at 24h for 0.5g/L concentration while the minimum corrosion rate is 0.305 mmpy at 120h at the same 0.5g/L concentration. Considering the inhibition efficiency values obtained, it is obvious that the degree of surface coverage of the plant extract active constituents adsorbed on mild steel surface is not significant. Similar results have been reported elsewhere (Eyu, 2013).

As a result of the poor corrosion protection of the plant extracts in alkaline environment, there have been works that evaluates the performance of other biomass extracts by synergism with the addition of materials like ions, salts and polymeric materials to see how they can synergistically improve the performance of the extracts either by improving the reactiveness between the inhibitor solution and the metal coupon or by stabilizing the active components of the extracts over time recording little or no nutrient degradation with time. For this reason, ZS was employed to evaluate the effect of synergism on the protection against deterioration of *OG* biomass extracts. In Figure 2 it was obvious that the rate of corrosion of the coupon was much higher in the blank environment. It was also, observed that at all concentrations of ZS (See Figure 2a) and OG (See Figure 2 b) the inhibitors were able to afford some level of inhibition.

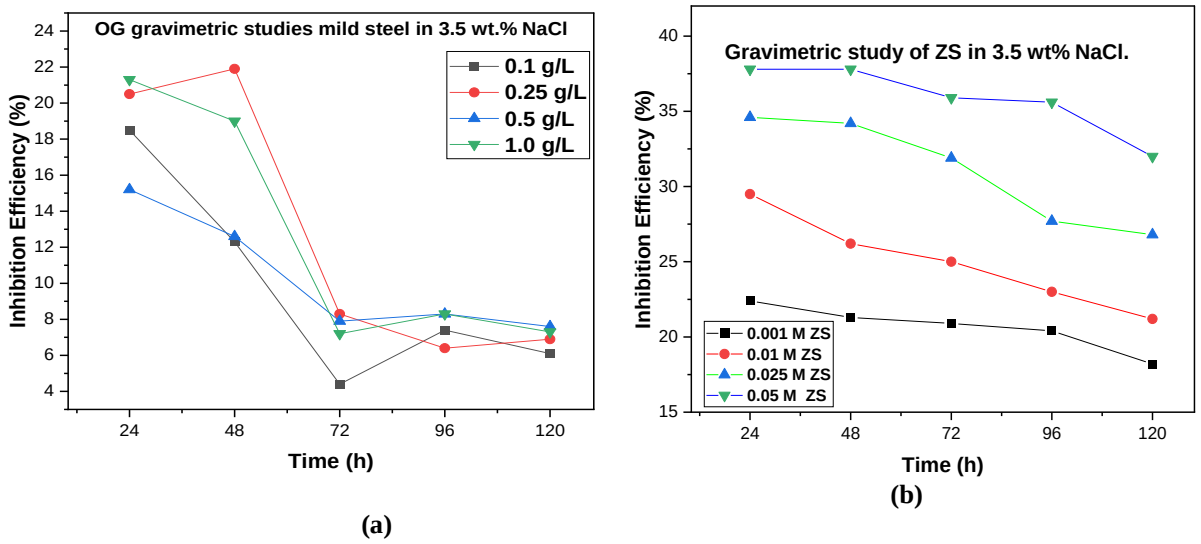


Figure 1. Variation of inhibition efficiency with time for: **(a)** OG inhibitor and **(b)** ZS in 3.5 wt.% NaCl.

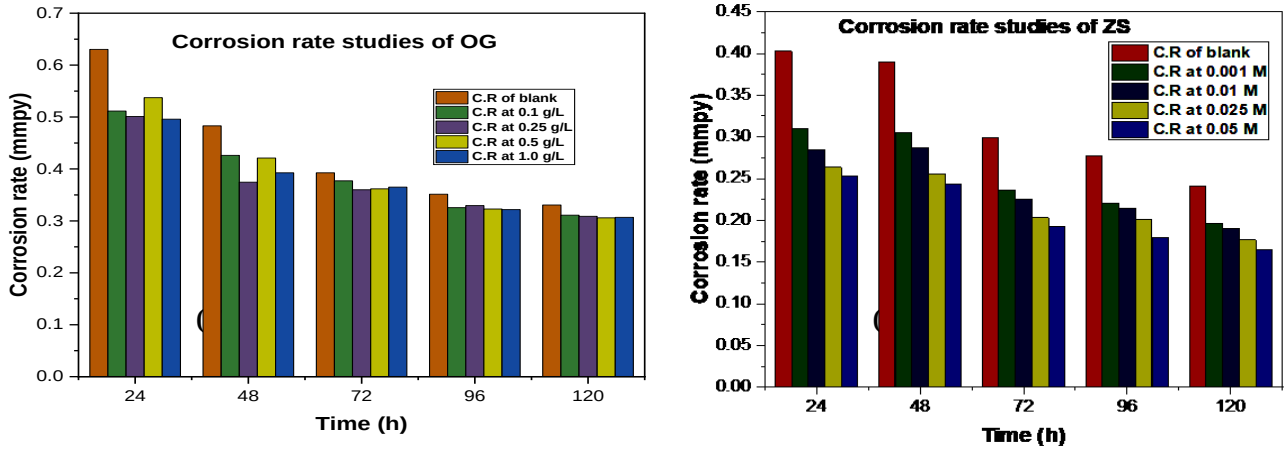
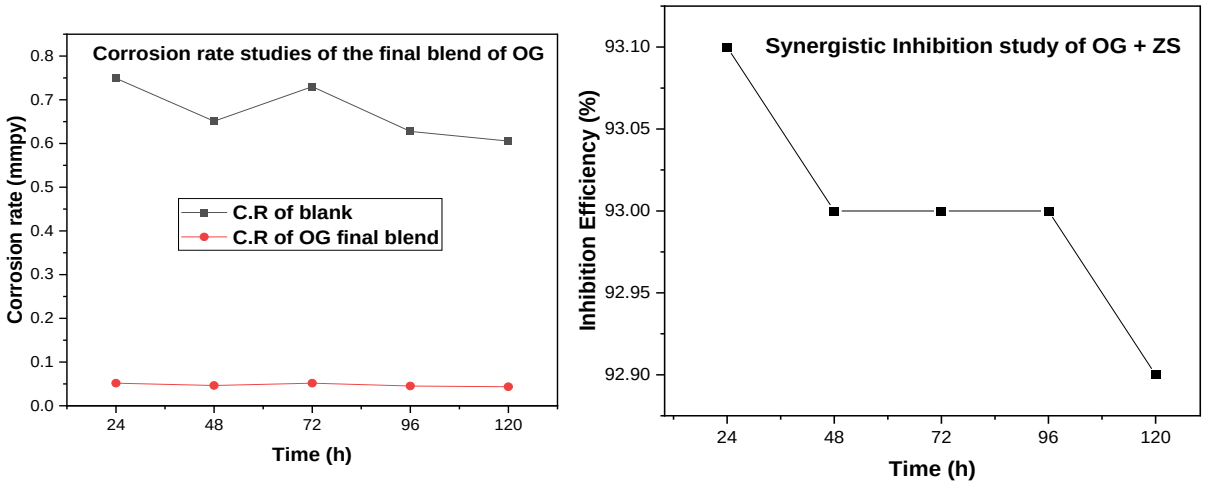


Figure 2. Variation of corrosion rate with time for: (a) OG inhibitor and (b) ZS in 3.5 wt.% NaCl.

The optimum corrosion rate recorded was 0.3099 mmpy at 24 h for 0.001 M concentration of ZS while the minimum corrosion rate was recorded seen as 0.1643 mmpy at 120 h for 0.05 M concentration. The result is presented in Figure 2.

3.1.4 Synergism of OG biomass with ZS

The optimal Synergism for OG are 0.25 g/L (OG) + 0.05 M (ZS) are seen in Table 1. The gravimetric study showed that the additive played a vital role in metal coupon protection against corrosion in 3.5 wt.% NaCl. The IE of OG follow the range; 93.1% > 93.0% = 93.0% > 92.9% = 92.9% for 24 h, 48 h, 72 h, 96 h and 120 h immersion time, respectively. It is expected that the metal surface should be covered by the inhibitor's active constituents resulting to a blockage between the substrate and the electrolyte. The rate of corrosion study showed that the blank increases with time whereas that of the blend remains almost stable with time (See Figure 3b).



(a) (b)

Figure 3a: The corrosion rate graph of the synergism between OG and ZS.
Figure 3b: The inhibition efficiency graph of the synergistic study between OG and ZS

3.2 Synergistic Index (SI)

The equation presented in Eq. 5 is usually obtained to calculate the type of reaction/interaction/synergism existing between two compounds, with this, one will be able to determine whether there is a cooperative synergism or competitive. Therefore, the type of synergism that exists between the biomass extract (OG) and the corresponding additives were assessed using this method with the outcome shown in Table 1.

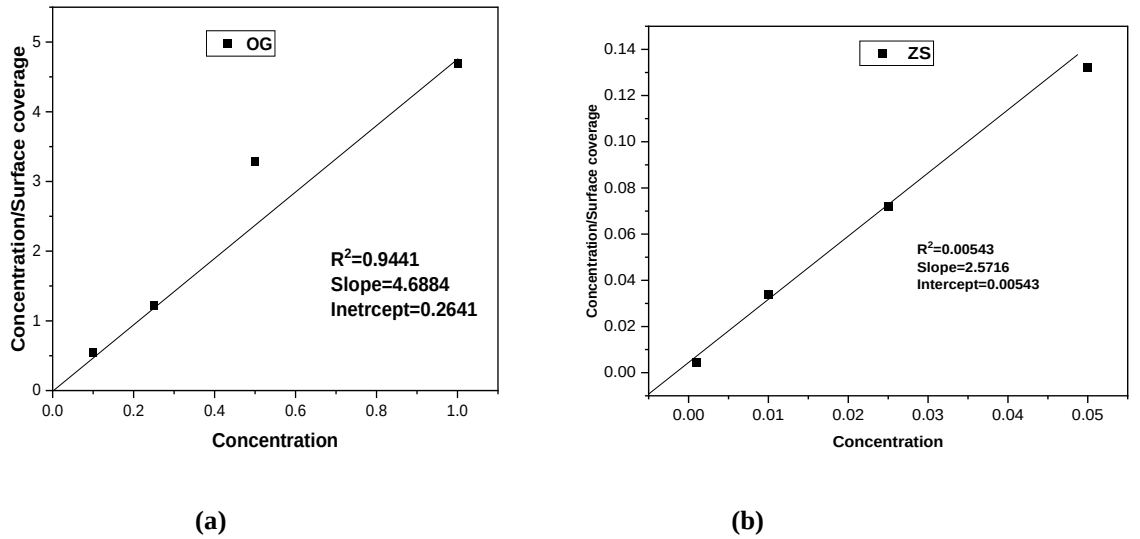
Table 1. Synergistic Index for the OG extract and the corresponding additives

Duration (h)	**OG + ZS** (*Ocimum gratissimum and zinc salt*)
24	0.503
48	0.501
72	0.472
96	0.469
120	0.419

The synergistic index measures the type of interaction between the compounds that are mixed in a system and same environmental condition. The synergism between OG + ZS yielded an index within the range of 0.419 to 0.503 for the corresponding immersion periods of 24 -120 h thus, suggesting a cooperative synergism among the blends.

3.3 Adsorption Studies

The behavior of the biomass extract under adsorption and the individual additive were studied using Eq. 6 and the results were obtained after the 24 h immersion period. The plotted graphs, Figure 4 a & b showed a coefficient of regression value very close to unity establishing a straight-line fitting thereby obeying the Langmuir isotherm of adsorption represented by the Eq. 6. The Langmuir isotherm makes the assumption that there is a linear relationship between the concentration of the inhibitor and the amount of metal surface coverage it provides. Additionally, it implies that during the adsorption process, the corrosion inhibitor merely adsorbs as a monolayer with negligible inhibitor-inhibitor interaction. The ranges of the obtained regression coefficient indicate that the corrosion inhibitors have active sites for reaction and adsorbed on the metal substrate's surface. The adsorbed species forms a thin layer that prevented the ingress of the corrosive species, hence the obtained inhibition efficiency values observed. In summary, the regression coefficient values obtained validates the obtained inhibition efficiency values.



(a) **(b)**

Figure 4. Langmuir adsorption isotherm plot for OG and ZS inhibitors, respectively.

3.4 Gas Chromatography- Mass Analysis (GC-MS):

This technique involved the characterization leaf extract of OG using GC-MS. The GC-MS evaluation was to ascertain the nature of the phytochemical compounds present in the extracts so as to predict their potency in corrosion inhibition studies. From the retention peaks and the corresponding spectral (Figure 5) matching with the library, the following information such as compound names, chemical formula, chemical structures, and percentage composition of OG were obtained. The major objective of performing GC-MS analysis is to ascertain the phytochemical constituents of a material. The biomass extracts are multi-component materials with different sub-components at varying percentage composition using the mass spectrometer (Jain *et al.*, 2016). Plant extracts have proved to be useful as good corrosion inhibitors, they are also, environmentally friendly. Figure 5 shows the evaluation of OG, as can be seen, there are about 27 peaks, indicating the existence of 27 different compounds in the biomass extract.

Table 2 shows the selected compounds that were present in OG with their retention time and percentage composition. The compounds through this study showed that they contain either of the following groups: Alkaloid, Flavonoids Tannin & Phenolic Compounds, Terpenoid and Saponin which demonstrates a promising inhibitory action from these active constituents, (Divya et al., 2019; Ikpeseni et al., 2021; Kalaichelvi & Dhivya, 2017; Madjouko et al., 2019). Alkaloids act as both nitrogen storage tanks and shield the metal from environmental damage. In a corrosive solution, alkaloids, which are aromatic hydrocarbons with nitrogen as a hetero element in the ring structure, are what bond with the coupon surface and prevent metals from corroding. (Garai *et al.*, 2012). As a result, some OG extract ingredients chemically adsorb on the mild substrate surface. and have a controlling effect on the extract's ability to inhibit corrosion. This explains the extract's reported slow rate of adsorption in NaCl solution containing 3.5 weight percent. Chemisorbed molecules are predicted to provide more potent protection because they reduce the metal's inherent reactivity at the sites where they bind.

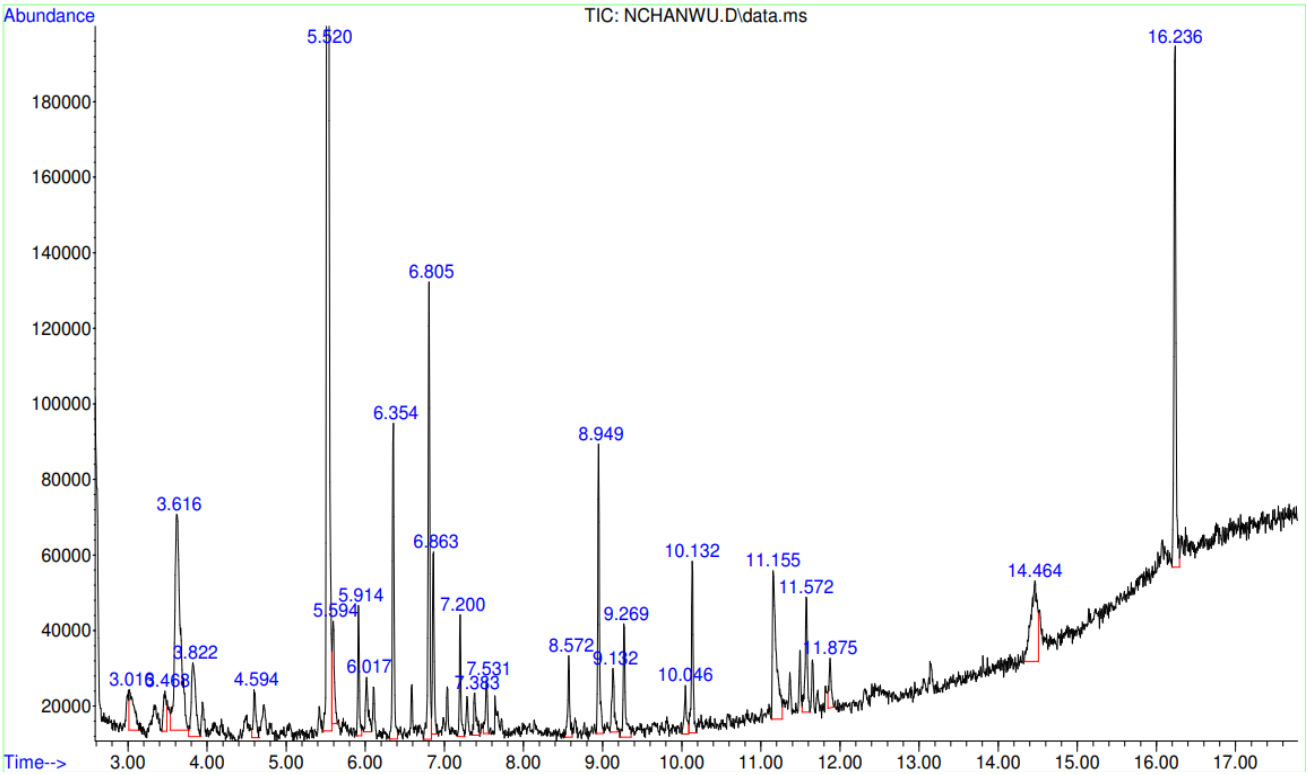
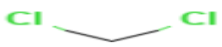
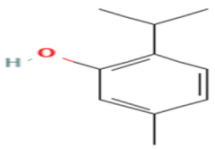
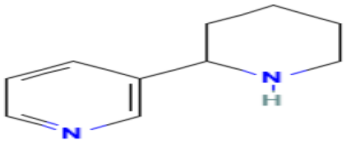
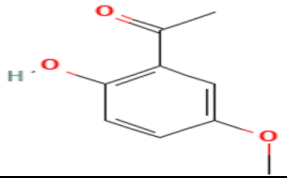


Figure **5.** GC-MS generated results for *Ocimum gratissimum* mass spectrometer.

Table 2. The most pronounced species identified in Ocimum gratissimum extract from the GC-MS analysis.

S/N	Name	Formula	Structure	Retention Time.	% composition
1	Methylene chloride	CH_2Cl_2		1.947	84.63
2	Benzene, 1-methyl-3-(1-methylethyl)-	$C_{13}H_{20}$		3.616	1.15
3	Thymol	$C_{10}H_{14}O$		5.520	6.10
4	Anabasine	$C_{10}H_{14}N_2$		6.017	0.13
5	Ethanone, 1-(2-hydroxy-5-methoxyphenyl)-	$C_9H_{10}O_3$		7.383	0.11

6	Pyrrolidine, 2-butyl-1-methyl-	$C_{19}H_{19}N$		1.907	1.02

3.5 Ultraviolet-Visible Spectroscopy result of OG

This study evaluates the stability of the OG biomass extract over time, it ascertains if and when the inhibitor solution degrades or precipitates during the gravimetric studies.

For aged extract of OG, the UV-analysis reveals the presence of the following peaks 610 nm, 537 nm, 627 nm, 575 nm and 524 nm and they were recorded with absorbance values of 1.9, 1.6, 1.6, 1.0 and 1.2 respectively. For the freshly prepared OG solution UV-analysis, the following peaks were recorded; 666 nm, 609 nm and 537 nm with absorbance values of 1.5, 0.4 and 0.4 respectively. There is a degradation of constituents and/or formation of new ingredients with time as seen by the different peaks present in a compound as a fresh extract and as an aged solution. This accounts for the reduction in the efficiency in inhibition of the OG extract in gravimetric studies as well as fall and rise in inhibition efficiency at different immersion period. (Kalaichelvi & Dhivya, 2017).The emergence of one or more peaks in the region between 200 and 400 nm in the UV-VIS spectra makes unsaturated groups and heteroatoms like S, N, and O easily identifiable, (Kiruthikajothi & Chandramohan, 2015; Njoku *et al.*, 2013). The findings demonstrate that organic chromophores are present in the biomass extracts. However, the inherent hurdles of designating the absorption peaks to specific system components impede the application of UV-visible spectrophotometry in the investigation of complex media. As previously noted, the results of UV-VIS analysis were confirmed by a number of analytical techniques, including GC/MS, to enable precise extract characterization and constituent identification, (Abbed et al., 2019). Peaks with wavelengths between 236 and 676 nm indicate the presence of alkaloids in the extracts. It is evident that the extract contains some of the alkaloids, flavonoids, etc discussed earlier. (Karpagasundari & Kulothungan, 2014). The UV-VIS study of the OG final blends showed that the blend retained all their constituents at 24 h through 120 h as shown in Figure 6. The observed phenomenon validated the gravimetric results of the final inhibitor blend

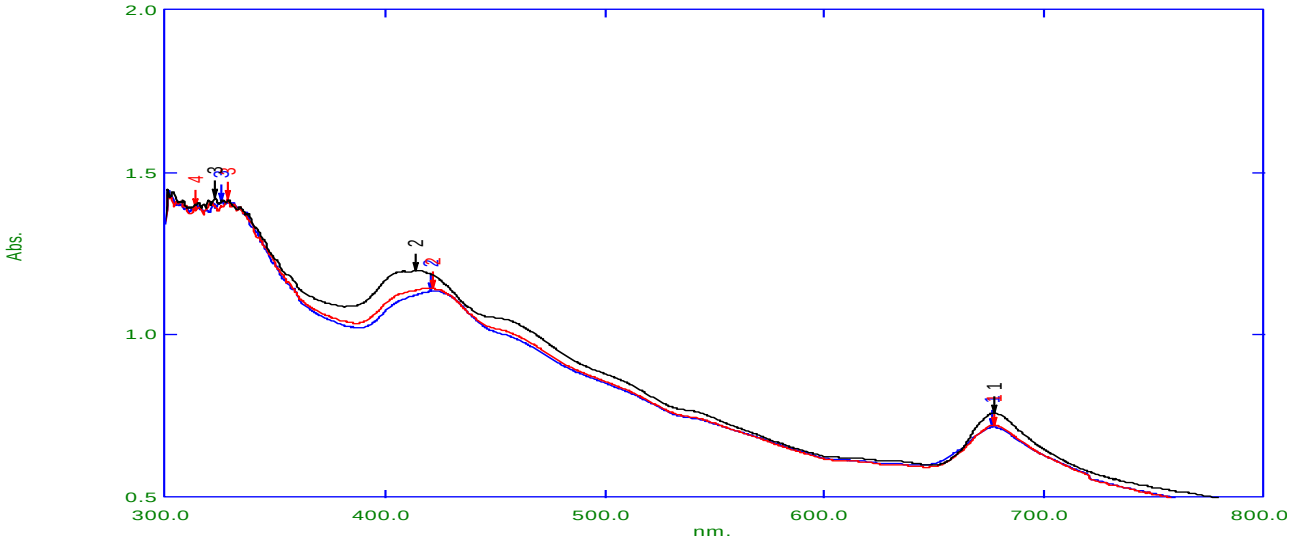


Figure **6.** UV study of the inhibitor blends of OG at 24 h, 72 h and 120 h during the gravimetric studies.

3.6 Fourier Transform Infrared Spectroscopic results

Using this approach, it was observed that the OG extract contains alcohol groups as O-H bond appeared as a powerful, wide band enclosing the span from 3000-3700 cm^{-1}. From the peaks, the maximum peak recorded within the samples was at 3600 cm^{-1}.

All the inhibitors and their corresponding corrosion products also reveal that this functional group is present (Mahalakshmi *et al.*, 2020). The OG inhibitor, its synergism with the additives and the final blends showed the presence of Nitrile functional group at the range of 2109 cm^{-1} - 2374 cm^{-1}. This group showed a prominent band at 2100 - 2400 cm^{-1} caused by the C-N triple bond. They are stronger than alkynes because they are more polar.

OG and the corrosion products from OG + ZS revealed the presence of aldehyde and ketone functional group with their peak at 1688 cm^{-1} and 1710 cm^{-1}. They have carbonyl group which contains C=O functional group and showed a strong, prominent stake-shaped band which is as a result of the extremely polar C=O bond. (Wade,Jr., 2003). OG and its corrosion products also revealed the presence of carboxylic acid combining characteristics of ketones and alcohols as a result of the presence of O-H and the C=O bond with the peaks ranging between 2800-3500 cm^{-1} (Figure 7). They also revealed the presence of amides which combines the features of Amines and ketone possessing both the C=O and the N-H bonds displaying a sharp band in the leftmost region of the spectrum, within the range of 3100-3500 cm^{-1}. (Alexander, 2016). The above results confirmed the presence of OG functional groups adsorbed onto the metal's surface thus protecting it from corrosion.

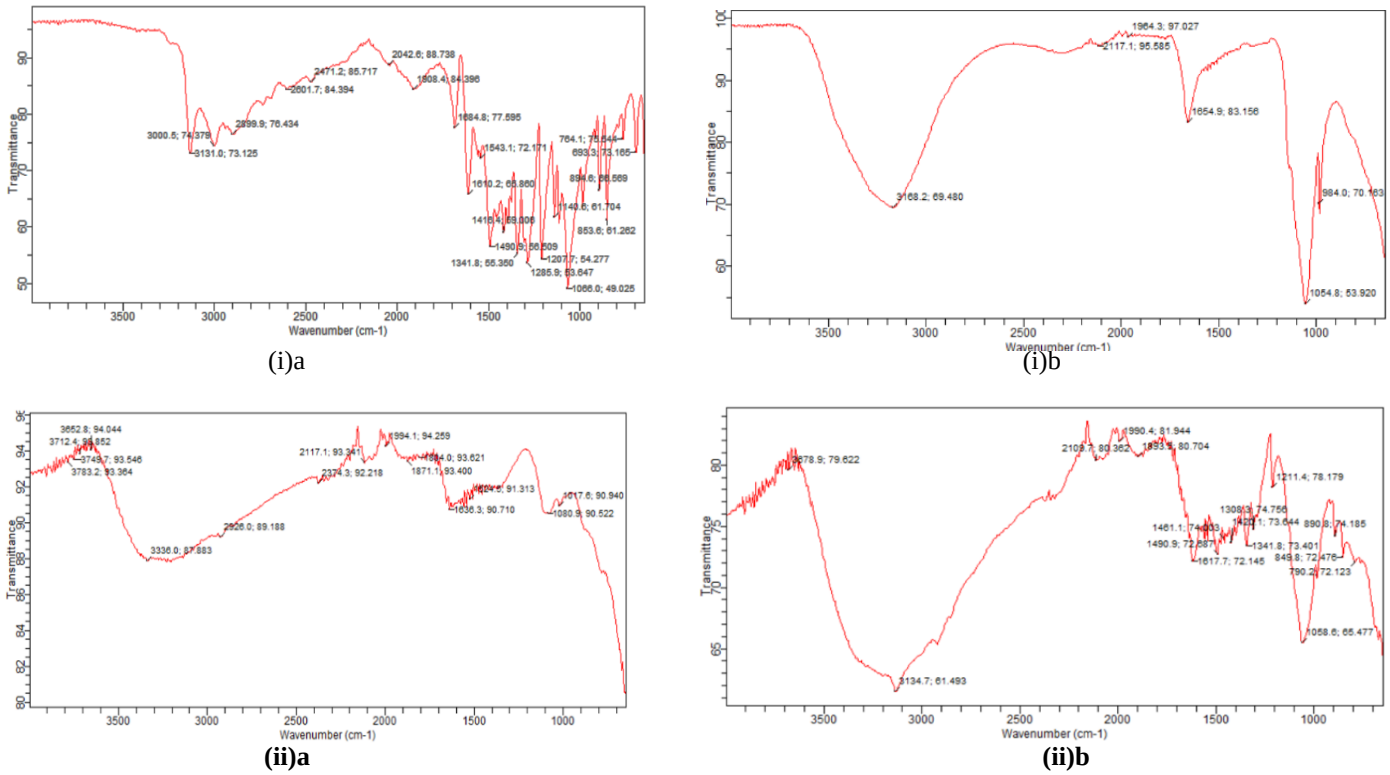


Figure 7**:** Shows the FTIR results of: (i) OG extract, and (ii) ZS inhibitors alone and with the scrapped corrosion products.

3.6 Computational Modelling of the selected active components of the *OG* extracts

3.6.1 Quantum Chemical Calculations

The selected molecular structure of OG are presented in Figure 8. The molecular structure, optimized geometry structure, density of electron distribution of highest occupied molecular orbital (HOMO) see Figure 9 and lowest unoccupied molecular orbital (LUMO), see Figure.10, Electrophilic, nucleophilic and radical parameters of the selected compounds present in OG extract were determined. They selected structures were density functional theory-optimized (DFT) with Dmol3 tools. After optimization, the energy of (E_{HOMO}), the energy of (E_{LUMO}), energy gap ($\Delta E = E_{LUMO} - E_{HOMO}$), Electronegativity, Global Hardness and Electron charge transfer were calculated and the obtained results presented in Table 3. It is evident that the benzene ring serves as the active site of adsorption since the electron density distributions of the HOMO and LUMO are equally distributed on the ring. (Wang *et al.*, 2020). The molecule's HOMO and LUMO orbitals, respectively, are connected to its capacity to give and take electrons. The molecule's strong capacity to donate electrons was shown by its high E_{HOMO} value, while its easier ability to absorb electrons was indicated by its low E_{LUMO} value. (Tabatabaei majd *et al.*, 2019). As a result, good corrosion inhibition efficacy results from easy electron transport between the inhibitor molecules and the metal surface when the inhibitor molecules have a high E_{HOMO} and a low E_{LUMO}, (Nwankwo *et al.*, 2021). Since ΔE measures a molecule's stability, lower values suggest that a molecule may be absorbed more readily on a metal surface. (Majd *et al.*, 2020). The compounds of OG have lower ΔE value ranging from 2.4473 eV to 6.1178 eV, correlating with its improved corrosion protection characteristics with the blends. The Koopman theorem states that Eq. 7 included the ionization potential (I) and

electron affinity (A) associated with the inhibitor molecule's EHOMO and ELUMO. The efficiency in inhibition as a result of electron donation is correlated with the absolute electronegativity (X) defined in Eq. 8, global hardness (γ) defined by Eq. 9, the value of ΔN and the fraction of electrons transported from the inhibitor to the metal surface (ΔN) as provided by Eq. 7.

The relation existing between ΔE and hardness has apparent physical importance. An electronic system with a high hardness is more stable than one with a lower hardness because stable molecular structures have a high ΔE. According to the relationship between X and ΔN, the molecule is more inclined to accept electrons and has a lower ability to emit them when X is higher. Since ΔN is below 3.6, the metal substrate surface's ability to donate electrons is increased and the inhibitor efficiency rises accordingly. (Asadi *et al., 2020)*. From Table 3, The range of ΔN values for OG compounds is 0.4891 to 1.1669, suggesting that these inhibitors have the ability to contribute electrons to the metal surface, promoting the development of coordinating bonds and an adsorption protective coating. (Aribo *et al.*, 2020).

Table 3: Table showing the selected compounds of *OG* and the calculated HOMO, LUMO, Energy gap, Electronegativity, Hardness and electron charge transfer values.

S/N	Compound	HOMO (ev)	LUMO(ev)	Energy gap (Δe)	Electronegativity (X)	Hardness (ɲ)	Electron Charge Transfer (ΔN)
1	Methylene Chloride	-7.0676	-0.9559	6.1178	4.0116	3.0559	0.4891
2	Benzene 1-methyl-3-(1-methyl ethyl)	-5.4979	-0.7894	4.7085	3.1467	2.3565	0.8176
3	Thymol	-5.1388	-0.7753	4.3653	2.9571	2.1818	0.9265
4	Anabasine	-5.1289	-1.5306	3.5983	3.3298	1.7992	1.0199
5	Ethanol 1-(2-hydroxy-5-mthoxy phenyl)	-5.3956	-2.9483	2.4473	4.1719	1.2237	1.0199
6	Pyrrodlidine, 2-butyl-1-methyl	-4.7439	-1.3606	3.3833	3.0523	1.6916	1.1669

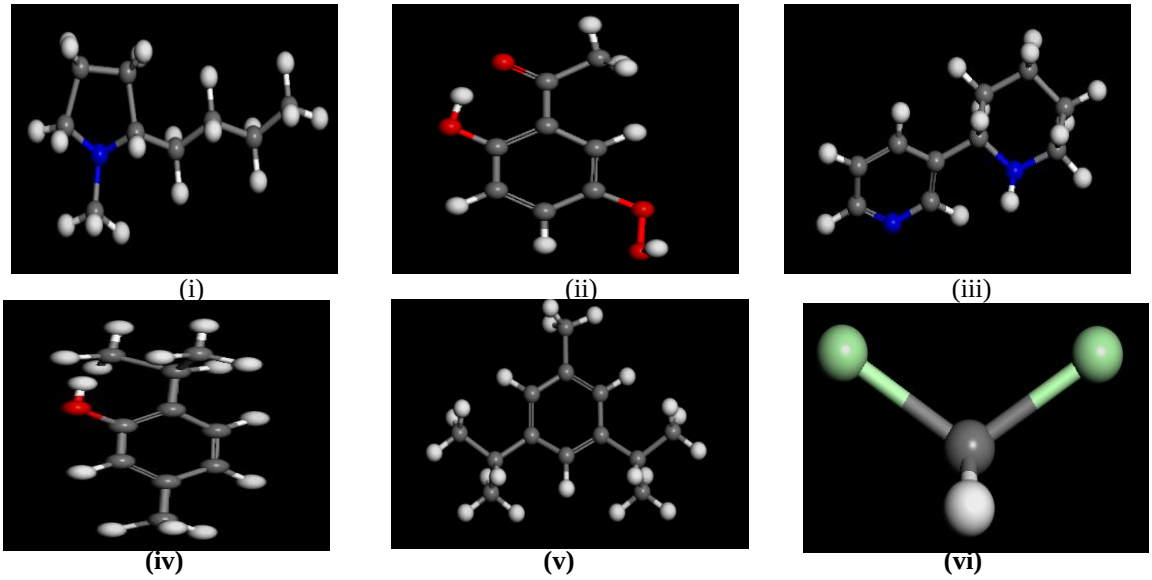


Figure **8.** Shows the modelled selected compounds present in OG extracts namely; (i) Pyrrodlidine, (ii) Ethanol 1-(2-hydroxy-5-methoxy phenyl), (iii) Anabasine, (iv) Thymol, (v) Benzene 1-methyl-3-(-1-methyl ethyl), and (vi) Methylene Chloride), respectively.

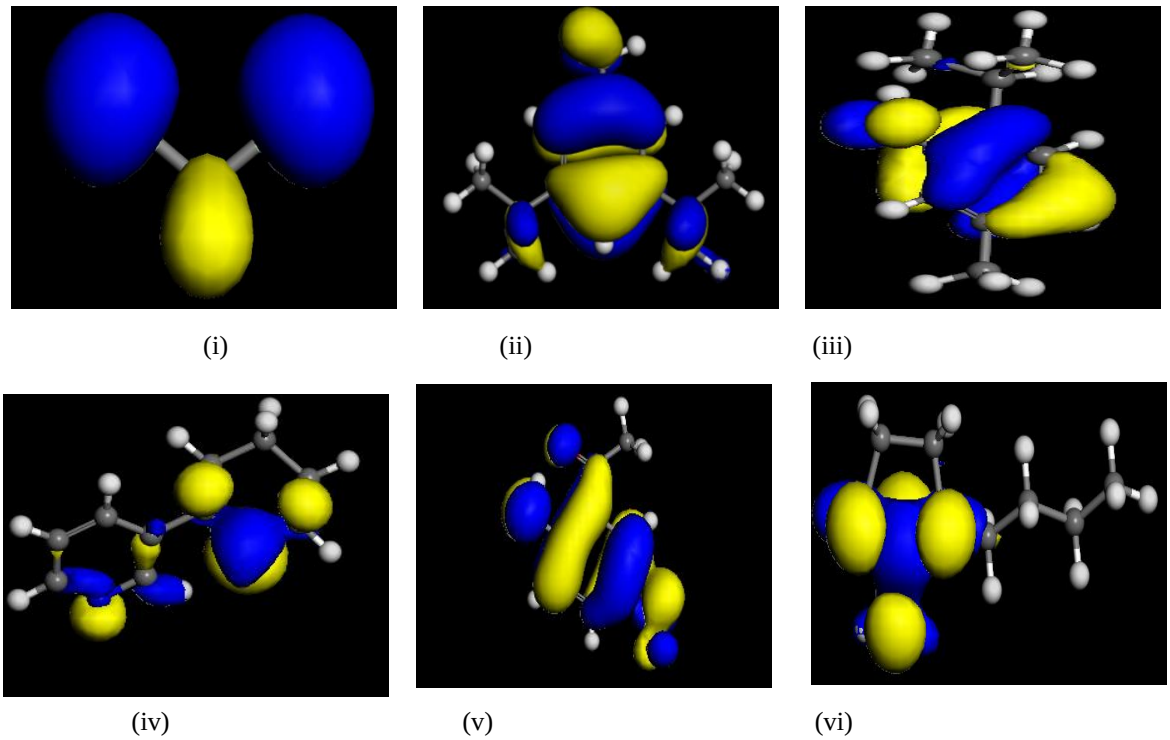


Figure **9.** Shows the modelled HOMO function of the compounds present in OG; (i) Methylene Chloride, (ii) Benzene 1-methyl-3-(-1-methyl ethyl), (iii) Thymol, (iv) Anabasine, (v) Pyrrodlidine, (vi) Ethanol 1-(2-hydroxy-5-methoxy phenyl), respectively.

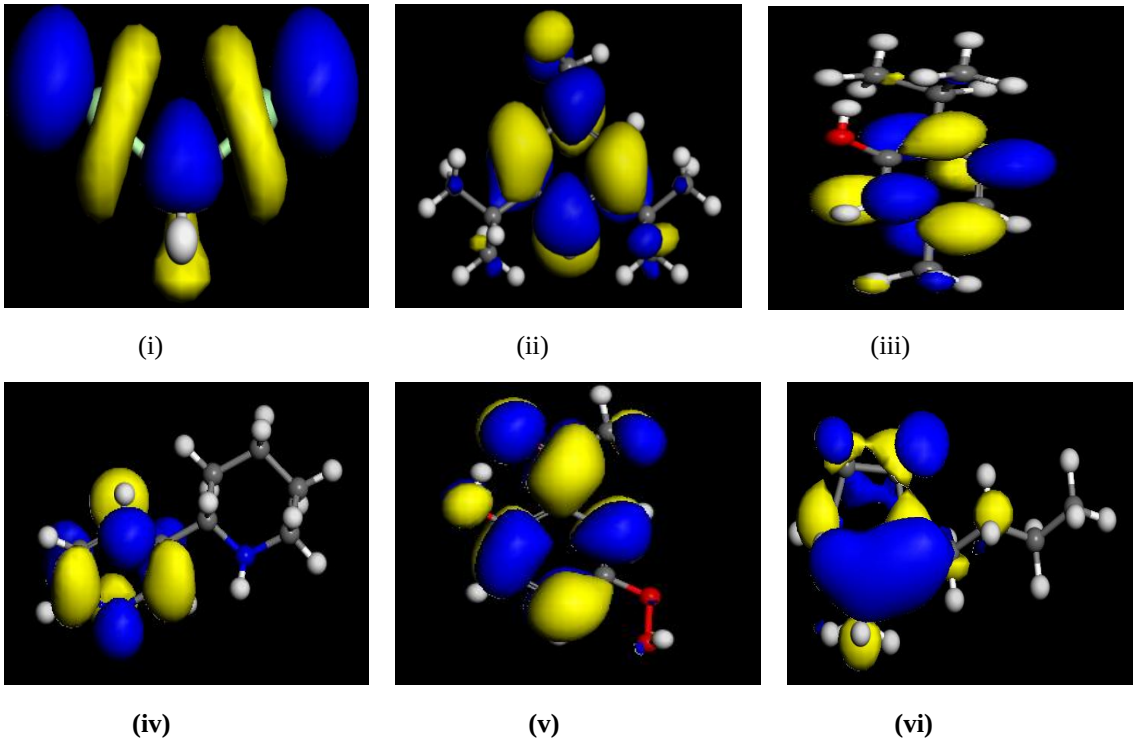


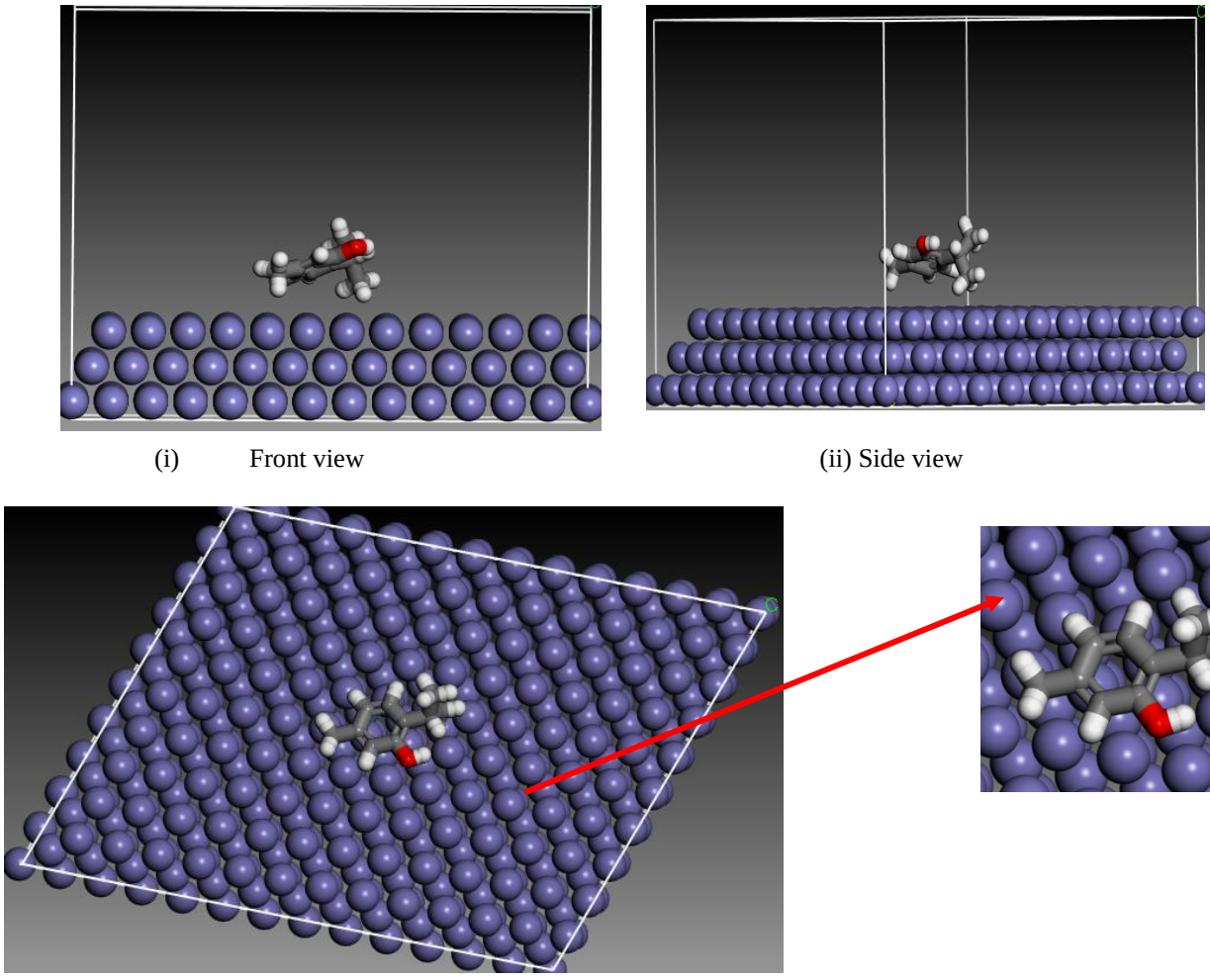
Figure **10.** Shows the modelled LUMO function of the compounds present in OG extract: (i) Methylene Chloride, (ii) Benzene 1-methyl-3-(-1-methyl ethyl), (iii) Thymol, (iv) Anabasine, and (v) Pyrrodlidine, (vi) Ethanol 1-(2-hydroxy-5-methoxy phenyl), respectively.

3.6.2 Molecular Dynamic Simulation

To simulate the impact of solvent on the inhibitor-metal interaction, the compound's adsorption on the steel surface was quantified using the Forcite simulation on Fe (110) crystal phase of steel. Figure 11 to 14 reflect that in each case the compounds adopt a flat lying orientation for adsorbing onto the metal surface. (Chaouiki *et al.*, 2020). The adsorbing energy (expressed in KJ/m) generated from the simulation results showed a range of values listed in Table 4. It's feasible that the inhibitor molecules will group together and adsorb on the metal surface to create a thick layer of molecules that will keep the metal surface and the water molecules apart and cause the observed corrosion inhibition, (Wang *et al.*, 2020). The adsorption strength follows the sequence. Benzene 1-methyl-3-(1-methyl ethyl) > Ethanol 1-(2-hydroxy-5-mthoxy phenyl) > Methylene Chloride > Anabasine > Thymol > Pyrrodlidine, 2-butyl-1-methyl. From the results it is expected that Benzene 1-methyl-3-(1-methyl ethyl) contributed significantly to the overall inhibition efficiency observed.

Table 4. Calculated adsorption energy for selected OG compounds

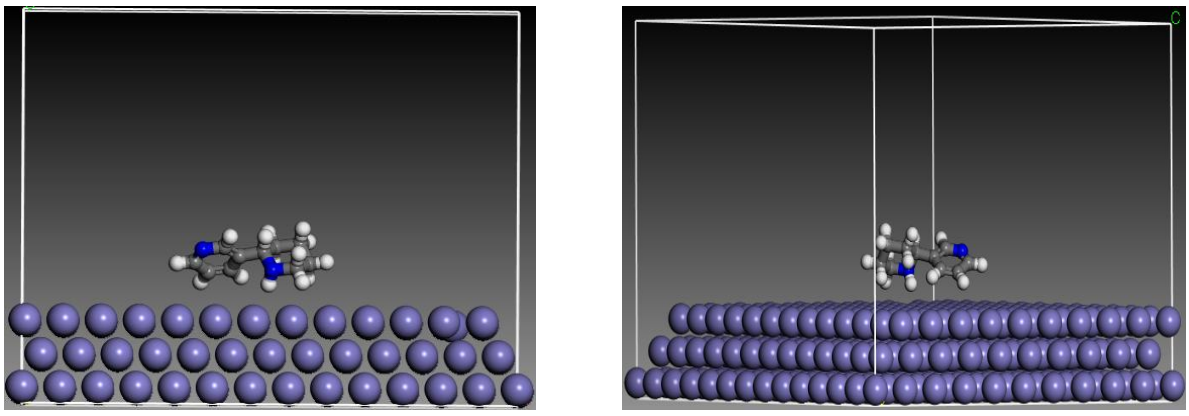
S/No	Compound	Adsorption Energy (KJ/mole)
i	Methylene Chloride	-117.4
ii	Benzene 1-methyl-3-(1-methyl ethyl)	-261.5
iii	Thymol	-91.2
iv	Anabasine	-101.4
v	Ethanol 1-(2-hydroxy-5-mthoxy phenyl)	-138.1
vi	Pyrrodlidine, 2-butyl-1-methyl	-65.2



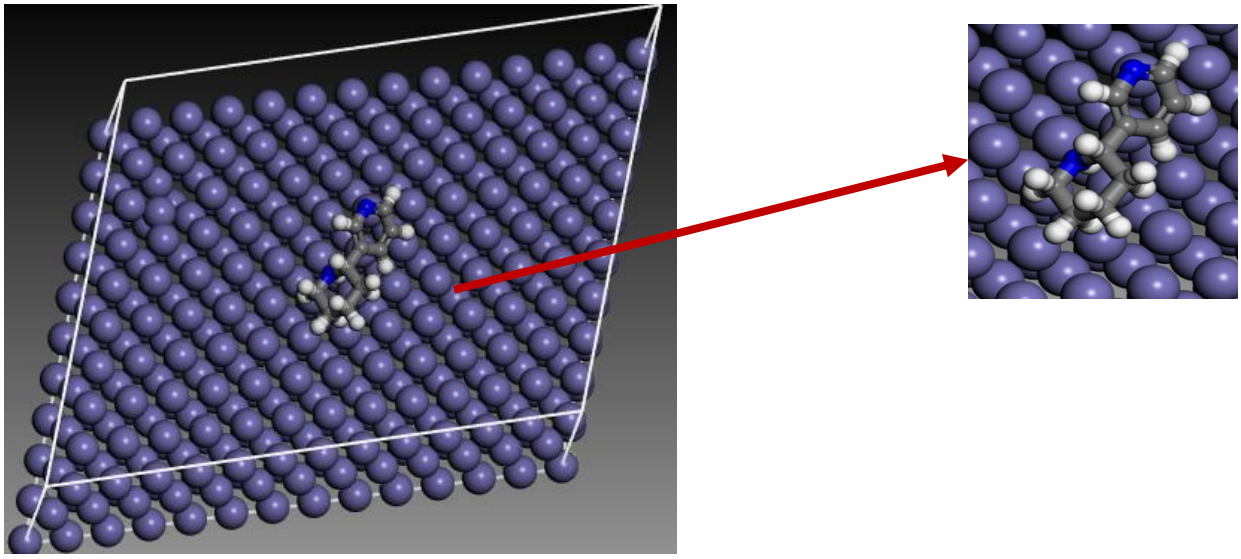
(i) Front view (ii) Side view

(iii) Top view

Figure **11.** Shows the: (i) Front topographic presentation, (ii) Side topography and (iii) Top view of thymol compound interacting with the Fe (110) surface.

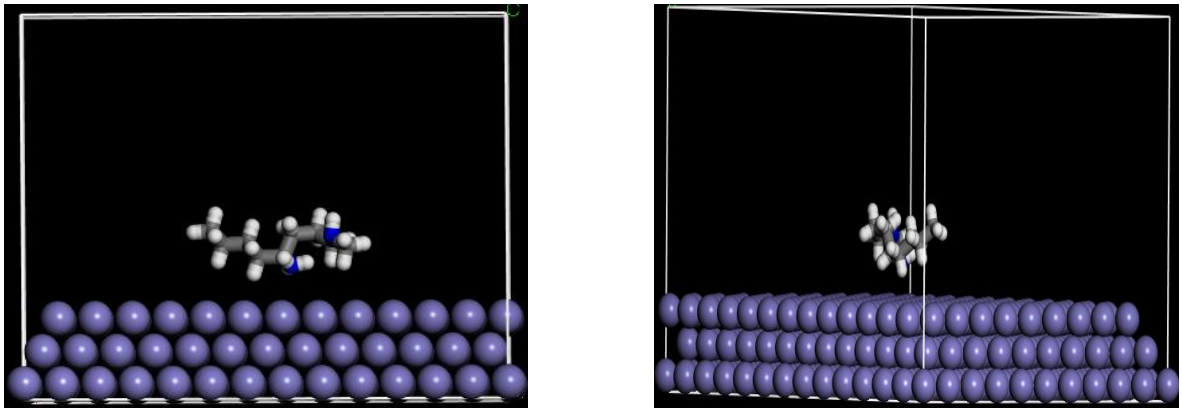


(i) Front view (ii) Side view

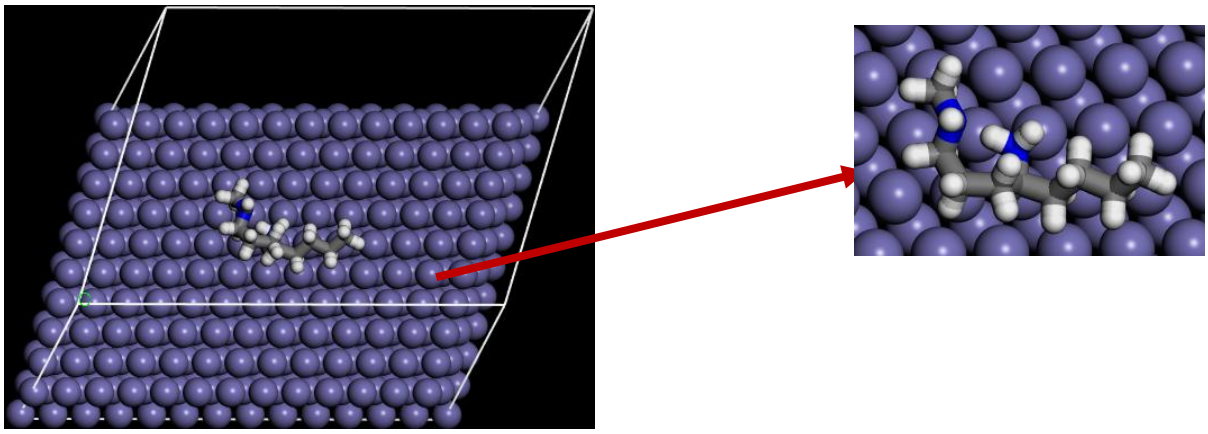


(ii) Top view

Figure **12.** Shows the: (i) Front topography (ii) Side topography and (iii) Top topography of Anabasine compound interacting with the Fe (110) surface.

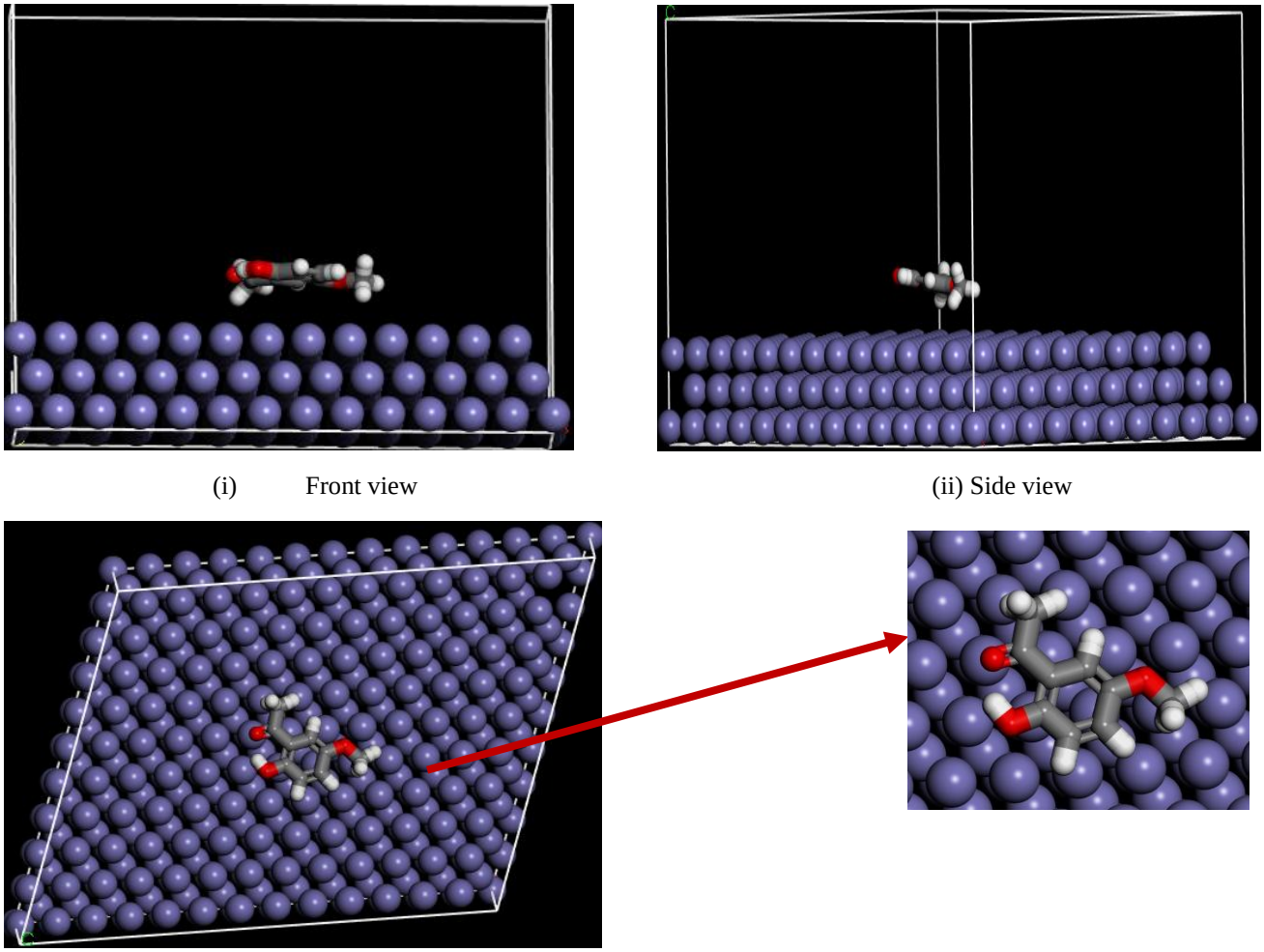


(i) Front view (ii) Side view



(iii) Top view

Figure **13.** Shows the: (i) Front view, (ii) Side view and (iii) Top view of Pyrrodlidine, 2-butyl-1-methyl compound interacting with the Fe (110) surface.



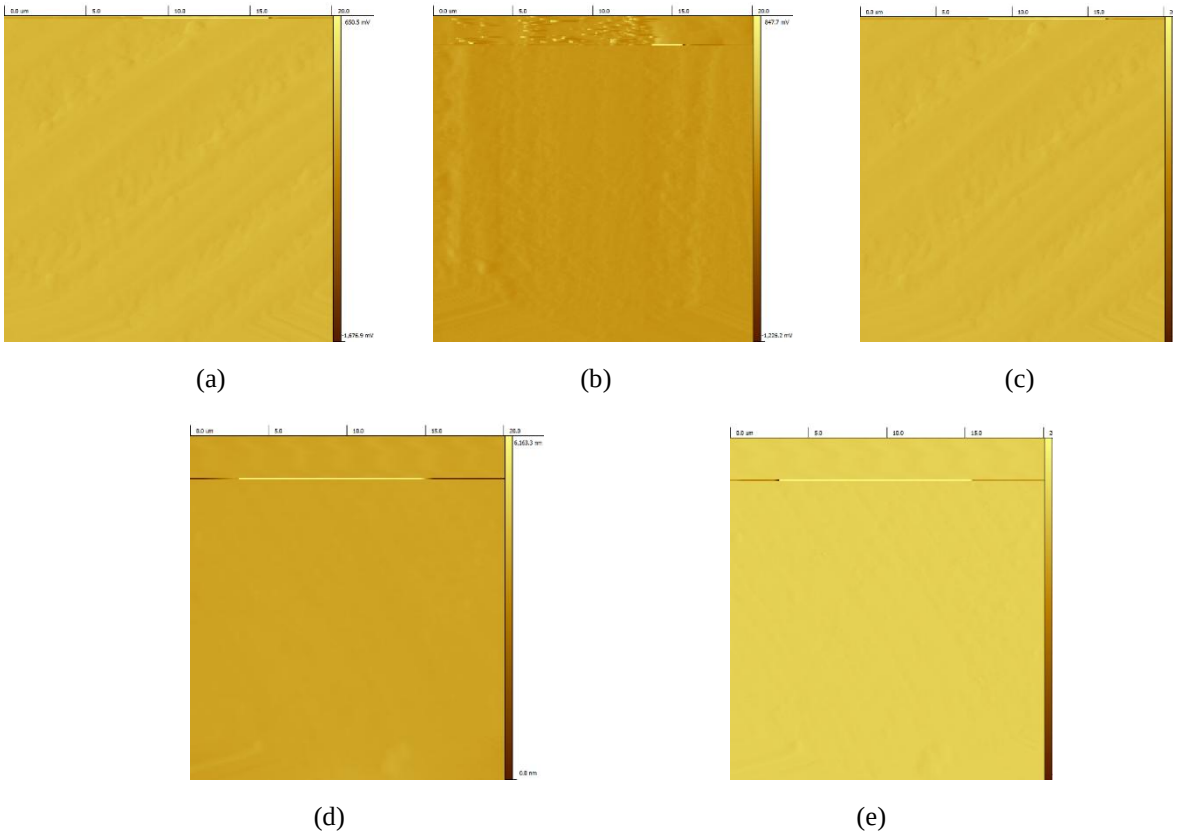
(i) Front view (ii) Side view

(iii) Top view

Figure **14.** Shows the: (i) Front topography, (ii) Side topography and (iii) Top topography of Ethanol 1-(2-hydroxy-5-mthoxy phenyl) compound interacting with the Fe (110) surface.

3.7 Atomic Force Microscopy Studies

After immersion in the uninhibited solution, the AFM results revealed a rough surface morphology; this could be because the mild steel underwent active dissolution in this environment. (See Figure 15a and 16a). The corrosion damage is shown to have decreased by the addition of OG extract, and mild steel surfaces in corrosive environments exhibit adsorbent species, which encourages the adsorption of OG components. This can be likened to the study carried out by (Blessing *et al.*, 2017) where OG extract inhibition effect was studied in a corrosive (acid) environment and the SEM study showed the coarseness of the coupon in the uninhibited system as a result of the corrosiveness of the environment while the introduction of OG inhibitor reduced the surface coarseness of the mild steel. Comparing Figure 15 and 16 it is evident that all the images in Figure 15 presents a rougher surface compared to their counterpart image in Fig. 16. Furthermore, the image presented in Figure 16f presents the most protected image of the metal surface due to the effect of the blend OG + ZS unlike what is obtainable with other surfaces immersed in the presence of OG and ZS separately. In Figure 16, the presence of adsorbent species were observed on the surface of the metals immersed in the inhibited solutions. The obtained result validates the experimental findings.

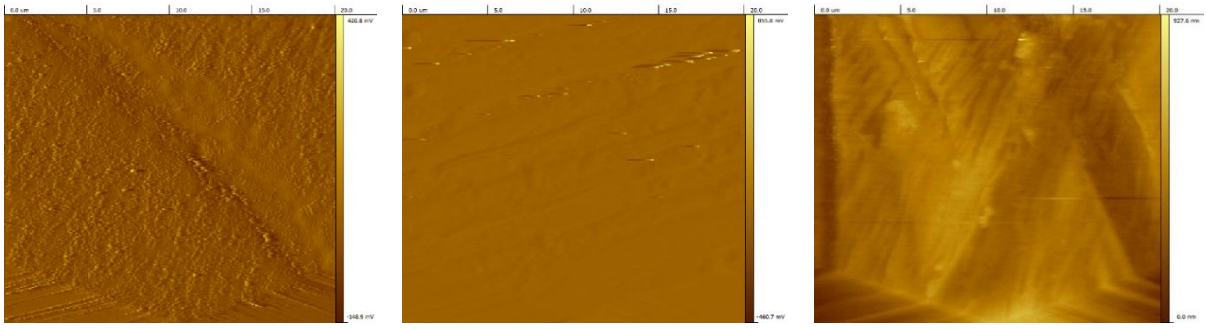


(a) (b) (c)

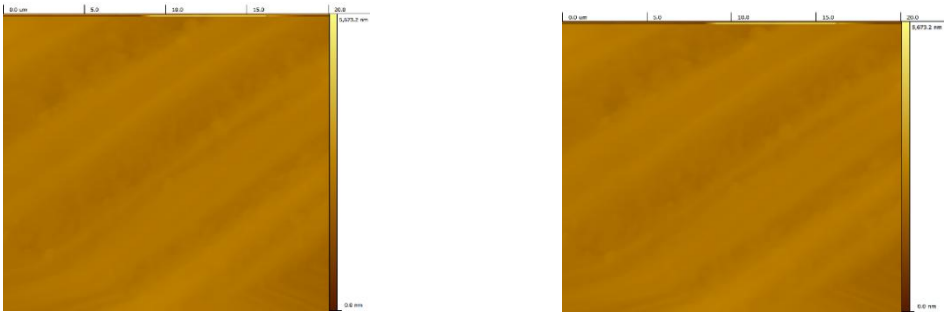
(d) (e)

Figure **15.** Shows the AFM topographic view of the coupon before immersion in the various inhibition systems.

(a) Topographic view of the mild steel in blank 3.5 % NaCl, (b) topographic view of the mild steel for OG extract in 0.25 g/L concentration in neutral solution (c) topographic view of the mild steel for OG extract in 1.0 g/L concentration in neutral solution (d) topographic view of the mild steel for ZS inhibitor in neutral solution (e) topographic view of the mild steel for OG + ZS synergism in neutral solutions.



(a) (b) (c)



(d) (e)

Figure **16.** Shows the AFM topographic view of the coupons after 24 h interaction with the various inhibitor systems.

(a) Topographic view of the mild steel in blank neutral system, (b) topographic view of the mild steel for OG extract in 0.25 g/L concentration in neutral solution (c) topographic view of the mild steel for OG extract in 1.0 g/L concentration in neutral solution (d) topographic view of the mild steel for ZS synergism in neutral solution (e) topographic view of the mild steel for OG +ZS synergism in neutral solution

Conclusion

The findings of the research show that the leaf extract of OG exhibits poor inhibition performance when used alone in the investigated environment (3.5% NaCl). The use of zinc ions proved to be efficient in boosting the stability and adsorption of the active ingredients of the biomass extracts as well as modifying the electrolyte system. The synergistic index of the biomass extract and the corresponding additives were less than 1 showing cooperative interaction between the extracts and the additive. The adsorption studies showed that the extracts and additive obeyed the Langmuir adsorption isotherm with regression coefficients close to unity. The Ultra-violet spectrum studies showed that the extract loses its chromophores and the formations of new peaks were observed with time until the additives were introduced which recorded stabilized peaks and absorbance value over immersion time. The GC-MS analysis showed that the leaf extract contains compounds with heteroatoms and pi-bonds like their conventional corrosion inhibitors which explain the recorded high inhibition efficiency. The identified compounds belong mostly to: alkaloid, flavonoids tannin & phenolic compounds, terpenoid and saponin which demonstrate a promising inhibitory action from these active constituents. The FTIR studies reveal the existence of functional groups present in OG crude extract. The presence of a protective film on the mild steel surface was observed, this could be due to the combined product species and organic species which emanates from the extract species. The computational studies showed the theoretical parameters like E_{LUMO}, E_{HOMO}, electronegativity, hardness, ionization energy, adsorption energy. The results indicate a promising interaction between the Fe (110) surface and the inhibitor molecule.

Author contributions

(a) Columbus L Ohia, Demian I Njoku, Maduabuchi .A. Chidiebere and Simeon C. Nwanonenyi Conceptualization; Methodology; Software; Investigation; Writing - original draft
(b) Emeka E. Oguzie Conceptualization; Methodology; Funding acquisition; Resources; Supervision; Writing - review & editing.
(c) Additionally, Benedict C. and Ben. I. Onyeachu, Formal analysis; Validation; Writing -review & editing.

Acknowledgment: The authors acknowledge the financial support from the World Bank Africa Centres of Excellence for Impact (ACE-Impact) Project (NUC/ES/507/1/304).

Disclosure statement: The authors declare that there are no conflicts of interest.
Compliance with Ethical Standards: This article does not contain any studies involving human or animal subjects.

References

Abbed, A. M., Al-Fartusie, F. S., Murtadha, M. K., Abdulsada, S. H., Farag, A. H., Ali, L. F. M., & Yasir, Y. A. (2019). Characterizations of lavender flowers extracts and study of their effects on peroxidase activity and some microorganisms. *Journal of Global Pharma Technology*, *11*(7), 181–191.

Adekanmi, D. G., & Olowofoyeku, A. E. (2020). African Star Apple: Potentials and Application of Some Indigenous Species in Nigeria. *Journal of Applied Sciences and Environmental Management*, *24*(8), 1307–1314. https://doi.org/10.4314/jasem.v24i8.1

Akalezi, C. O., & Oguzie, E. E. (2016). Evaluation of anticorrosion properties of Chrysophyllum albidum leaves extract for mild steel protection in acidic media. *International Journal of Industrial Chemistry*, *7*(1), 81–92. https://doi.org/10.1007/s40090-015-0057-5

Al Otaibi, N., & Hammud, H. H. (2021). Corrosion inhibition using harmal leaf extract as an eco-friendly corrosion inhibitor. *Molecules*, *26*(22). https://doi.org/10.3390/molecules26227024

Alam, P. N., Rosnelly, C. M., Karo karo, J. A., Ilhamdi, A., Soekarno, R., & Aslam, I. N. (2021). Utilization of Natural Extracts as Corrosion Inhibitors in the Seawater Environment. *Jurnal Rekayasa Kimia & Lingkungan*, *16*(2), 68–74. https://doi.org/10.23955/rkl.v16i2.18156

Alexander, P. (2016). Phytochemical Screening and Mineral Composition of the Leaves of Ocimum gratissimum (Scent Leaf). *International Journal of Applied Sciences and Biotechnology*, *4*(2), 161–165. https://doi.org/10.3126/ijasbt.v4i2.15101

Amar, H., Benzakour, J., Derja, A., Villemin, D., Moreau, B., & Braisaz, T. (2006). Piperidin-1-yl-phosphonic acid and (4-phosphono-piperazin-1-yl) phosphonic acid: A new class of iron corrosion inhibitors in sodium chloride 3% media. *Applied Surface Science*, *252*(18), 6162–6172. https://doi.org/10.1016/j.apsusc.2005.07.073

Amiery, A. A. Al, Mohamad, A. B., Kadhum, A. A. H., & Shaker, L. M. (2022). Experimental and theoretical study on the corrosion inhibition of mild steel by nonanedioic acid derivative in hydrochloric acid solution. *Scientific Reports*, 1–22. https://doi.org/10.1038/s41598-022-08146-8

Anupama, K. K., Ramya, K., & Joseph, A. (2016). Electrochemical and computational aspects of surface interaction and corrosion inhibition of mild steel in hydrochloric acid by Phyllanthus amarus leaf extract (PAE). *Journal of Molecular Liquids*, *216*, 146–155. https://doi.org/10.1016/j.molliq.2016.01.019

Aramaki, K. (2001). Treatment of zinc surface with cerium(III) nitrate to prevent zinc corrosion in aerated 0.5 M NaCl. *Corrosion Science*, *43*(11), 2201–2215. https://doi.org/10.1016/S0010-938X(00)00189-X

Aribo, S., Olusegun, S. J., Rodrigues, G. L. S., Ogunbadejo, A. S., Igbaroola, B., Alo, A. T., Rocha, W. R., Mohallem, N. D. S., & Olubambi, P. A. (2020). Experimental and theoretical investigation on corrosion inhibition of hexamethylenetetramine [HMT] for mild steel in acidic solution. *Journal of the Taiwan Institute of Chemical Engineers*, *112*, 222–231. https://doi.org/10.1016/j.jtice.2020.06.011

Asadi, N., Ramezanzadeh, M., Bahlakeh, G., & Ramezanzadeh, B. (2020). Theoretical MD/DFT computer explorations and surface-electrochemical investigations of the zinc/iron metal cations interactions with highly active molecules from Lemon balm extract toward the steel corrosion retardation in saline solution. *Journal of Molecular Liquids*, *310*, 113220. https://doi.org/10.1016/j.molliq.2020.113220

Authors, F. (2017). *An electrochemical investigation of azole derivative on aluminum in 0 . 25 M HCl solution using EN and EIS techniques*. https://doi.org/10.1108/ACMM-02-2015-1507

Baby, A. G., Rajendran, S., Johnsirani, V., Al-Hashem, A., Karthiga, N., & Nivetha, P. (2020). Influence of zinc sulphate on the corrosion resistance of l80 alloy immersed in sea water in the absence and presence of sodium potassium tartrate and trisodium citrate. *International Journal of Corrosion and Scale Inhibition*, *9*(3), 979–999. https://doi.org/10.17675/2305-6894-2020-9-3-12

Bahlakeh, G., Ramezanzadeh, M., & Ramezanzadeh, B. (2017). Experimental and theoretical studies of the synergistic inhibition effects between the plant leaves extract (PLE) and zinc salt (ZS) in corrosion control of carbon steel in chloride solution. In *Journal of Molecular Liquids* (Vol. 248). Elsevier B.V. https://doi.org/10.1016/j.molliq.2017.10.120

Blessing, A. C., Arinzechukwu, C. M., & Emeka, O. E. (2017). *Protecting Mild Steel from Acid Corrosion Using Extract from Ocimum gratissimum Leaves Protecting Mild Steel from Acid Corrosion Using Extract from Ocimum gratissimum Leaves*. *April*. https://doi.org/10.18052/www.scipress.com/ILCPA.73.9

Casaletto, M. P., Figà, V., Privitera, A., Bruno, M., Napolitano, A., & Piacente, S. (2018). Inhibition of Cor-Ten steel corrosion by "green" extracts of Brassica campestris. *Corrosion Science*, *136*, 91–105. https://doi.org/10.1016/j.corsci.2018.02.059

Chaouiki, A., Chafiq, M., Rbaa, M., Salghi, R., Lakhrissi, B., Ali, I. H., Bashir, S., & Chung, I. M. (2020). Comprehensive assessment of corrosion inhibition mechanisms of novel benzimidazole compounds for mild steel in HCl: An experimental and theoretical investigation. *Journal of Molecular Liquids*, *320*, 114383. https://doi.org/10.1016/j.molliq.2020.114383

Chidiebere, M. A., Oguzie, E. E., Liu, L., Li, Y., & Wang, F. (2015). Inhibitory Action of Funtumia elastica Extracts on the Corrosion of Q235 Mild Steel in Hydrochloric Acid Medium: Experimental and

Theoretical Studies. *Journal of Dispersion Science and Technology*, *36*(8), 1115–1125. https://doi.org/10.1080/01932691.2014.956114

Cotting, F., & Vieira, I. (n.d.). Octylsilanol and Ce (III) ions – alternative corrosion inhibitors for carbon steel in chloride neutral solutions. *Integrative Medicine Research*, *9*(4), 8723–8734. https://doi.org/10.1016/j.jmrt.2020.06.011

da Silva, J. P., da Silva, M. B., Campelo, S. R., Salgado, U. I., Diniz, J. A. P., Esterre, P., Rozental, S., & Salgado, C. G. (2010). TGF-β plasma levels in chromoblastomycosis patients during itraconazole treatment. *Cytokine*, *51*(2), 202–206. https://doi.org/10.1016/j.cyto.2010.05.004

Davis, G. D., Von Fraunhofer, J. A., Krebs, L. A., & Dacres, C. M. (2001). The use of tobacco extracts as corrosion inhibitors. *NACE - International Corrosion Conference Series*, *2001-March*(March).

Dehghani, A., Bahlakeh, G., Ramezanzadeh, B., & Ramezanzadeh, M. (2019). Electronic/atomic level fundamental theoretical evaluations combined with electrochemical/surface examinations of Tamarindus indiaca aqueous extract as a new green inhibitor for mild steel in acidic solution (HCl 1 M). *Journal of the Taiwan Institute of Chemical Engineers*, *102*, 349–377. https://doi.org/10.1016/j.jtice.2019.05.006

Divya, P., Subhashini, S., Prithiba, A., & Rajalakshmi, R. (2019). Tithonia diversifolia flower extract as green corrosion inhibitor for mild steel in acid medium. *Materials Today: Proceedings*, *18*, 1581–1591. https://doi.org/10.1016/j.matpr.2019.05.252

Doubi, M., Abbout, S., Erramli, H., Dermaj, A., Chebabe, D., & Touir, R. (2020). Performance of the novel corrosion inhibitor based on Cetamine to protect mild steel in surface water solution : electrochemical and surface studies. *Chemical Papers*, *2016*. https://doi.org/10.1007/s11696-020-01413-w

Eddy, N. O., Odoemelam, S. A., & Ama, I. N. (2010). Ethanol extract of Ocimum gratissimum as a green corrosion inhibitor for the corrosion of mild steel in H2SO4. *Green Chemistry Letters and Reviews*, *3*(3), 165–172. https://doi.org/10.1080/17518251003636428

El-hafez, G. M. A., & Badawy, W. A. (2013). Ac ce p d us t. *Electrochimica Acta*. https://doi.org/10.1016/j.electacta.2013.06.079

Eyu, G. D. (2013). *Effect of Vernonia Amygdalina Extract on Corrosion Inhibition of Mild Steel In Simulated Seawater*. https://www.researchgate.net/publication/281212449

Fawzy, A., Abdallah, M., Zaafarany, I. A., Ahmed, S. A., & Althagafi, I. I. (2018). NU SC. *Journal of Molecular Liquids*, *2017*, #pagerange#. https://doi.org/10.1016/j.molliq.2018.05.140

G, H. K., & O, J. A. (2017). Corrosion Inhibition of Mild Steel in Simulated Seawater by Nymphae Pubscens Leaf Extracts (NLE). *International Journal of Advanced Research in Chemical Science*, *4*(12), 32–40. https://doi.org/10.20431/2349-0403.0412004

Garai, S., Garai, S., Jaisankar, P., Singh, J. K., & Elango, A. (2012). A comprehensive study on crude methanolic extract of Artemisia pallens (Asteraceae) and its active component as effective corrosion inhibitors of mild steel in acid solution. *Corrosion Science*, *60*, 193–204. https://doi.org/10.1016/j.corsci.2012.03.036

Haddadi, S. A., Alibakhshi, E., Bahlakeh, G., Ramezanzadeh, B., & Mahdavian, M. (2019). A detailed atomic level computational and electrochemical exploration of the Juglans regia green fruit shell extract as a sustainable and highly efficient green corrosion inhibitor for mild steel in 3.5 wt% NaCl solution. *Journal of Molecular Liquids*, *284*, 682–699. https://doi.org/10.1016/j.molliq.2019.04.045

Hajar, H. M., Fakhratul, M., Zulkifli, R., Sabri, M., Ghazali, M., & Fitriadhy, A. (2016). *Lawsonia inermis performance as corrosion inhibitor for mild steel in seawater Perovskite-Based Varistor Ceramics View project THE DEVELOPMENT OF LAWSONIA INERMIS AS CORROSION INHIBITOR IN ACRYLIC COATING FOR ALUMINIUM ALLOY IN SEAWATER View project*. https://www.researchgate.net/publication/308592492

Ikhmal, W. M. K. W. M., Maria, M. F. M., Rafizah, W. A. W., Norsani, W. N. W. M., & Sabri, M. G. M. (2019). Corrosion inhibition of mild steel in seawater through green approach using leucaena leucocephala leaves extract. *International Journal of Corrosion and Scale Inhibition*, *8*(3), 628–643. https://doi.org/10.17675/2305-6894-2019-8-3-12

Ikhmal, W. M. K. W. M., Yasmin, M. Y. N., Maria, M. F. F., Syaizwadi, S. M., Rafizah, W. A. W., Sabri, M. G. M., & Zahid, B. M. (2020). Evaluating the performance of andrographis paniculata leaves extract as additive for corrosion protection of stainless steel 316l in seawater. *International Journal of Corrosion and Scale Inhibition*, *9*(1), 118–133. https://doi.org/10.17675/2305-6894-2020-9-1-7

Ikpeseni, S. C., Owamah, H. I., Owebor, K., Ameh, E. S., Sada, S. O., & Otuaro, E. (2021). Corrosion Inhibition Efficiency, Adsorption and Thermodynamic Studies of Ocimum Gratissimum on Carbon Steel in 2 M Sodium Chloride Solution. *Journal of Bio- and Tribo-Corrosion*, *7*(3). https://doi.org/10.1007/s40735-021-00505-8

Ivušić, F., Lahodny-Šarc, O., Ćurković, H. O., & Alar, V. (2015). Synergistic inhibition of carbon steel corrosion in seawater by cerium chloride and sodium gluconate. *Corrosion Science*, *98*, 88–97. https://doi.org/10.1016/j.corsci.2015.05.017

Jain, P. K., Soni, A., Jain, P., & Bhawsar, J. (2016). Phytochemical analysis of Mentha spicata plant extract using UV-VIS, FTIR and GC/MS technique. *Journal of Chemical and Pharmaceutical Research*, *8*(2), 1–6.

Kaghazchi, L., Naderi, R., & Ramezanzadeh, B. (2021). Synergistic mild steel corrosion mitigation in sodium chloride-containing solution utilizing various mixtures of phytic acid molecules and Zn2+ ions. *Journal of Molecular Liquids*, *323*. https://doi.org/10.1016/j.molliq.2020.114589

Kalaichelvi, K., & Dhivya, S. M. (2017). Screening of phytoconstituents, UV-VIS Spectrum and FTIR analysis of Micrococca mercurialis (L.) Benth. *International Journal of Herbal Medicine*, *5*(6), 40–44.

Karpagasundari, C., & Kulothungan, S. (2014). Analysis of bioactive compounds in Physalis minima leaves using GC MS, HPLC, UV-VIS and FTIR techniques. *~ 196 ~ Journal of Pharmacognosy and Phytochemistry*, *3*(4), 196–201.

Kermani, M. B., & Morshed, A. (2003). Carbon dioxide corrosion in oil and gas production - A compendium. *Corrosion*, *59*(8), 659–683. https://doi.org/10.5006/1.3277596

Khadija, G., Saleem, A., Akhtar, Z., Naqvi, Z., Gull, M., Masood, M., Mukhtar, S., Batool, M., Saleem, N., Rasheed, T., Nizam, N., Ibrahim, A., & Iqbal, F. (2018). Short term exposure to titanium, aluminum and vanadium (Ti 6Al 4V) alloy powder drastically affects behavior and antioxidant metabolites in vital organs of male albino mice. *Toxicology Reports*, *5*(June), 765–770. https://doi.org/10.1016/j.toxrep.2018.06.006

Kiruthikajothi, K., & Chandramohan, G. (2015). Corrosion inhibition of mild steel in hydrochloric acid solution by amino acid complexes. *Oriental Journal of Chemistry*, *31*(3), 1351–1354. https://doi.org/10.13005/ojc/310312

Lai, Y., Gao, Y., Jin, Y., & Wen, L. (2021). Study of methionine as green corrosion inhibitor for TWIP steel in neutral chloride solution. *Materials Research Express*, *8*(4). https://doi.org/10.1088/2053-1591/abf6fa

Loto, R. T., Fajobi, M., Oluwole, L., & Loto, C. A. (2020). Corrosion inhibition effect of calcium gluconate on mild steel in artificial seawater. *Cogent Engineering*, *7*(1). https://doi.org/10.1080/23311916.2020.1712155

Louadi, Y. E., Abrigach, F., Bouyanzer, A., Touzani, R., El Assyry, A., Zarrouk, A., & Hammouti, B. (2017). Theoretical and experimental studies on the corrosion inhibition potentials of two tetrakis pyrazole derivatives for mild steel in 1.0 M HCl. *Portugaliae Electrochimica Acta*, *35*(3), 159–178. https://doi.org/10.4152/pea.201703159

Madjouko, M. A., Tchameni, S. N., Tchinda, E. S., Dongmo Jazet, P. M., Kamsu, P. N., Medzue Souop Kamga, V. A., Sameza, M. L., Tchoumbougnang, F., & Menut, C. (2019). Inhibitory effects of essential oils from Ocimum basilicum and Ocimum gratissimum on Colletotrichum musae: The causal agent of bananas anthracnose. *Journal of Phytopathology*, *167*(5), 257–264. https://doi.org/10.1111/jph.12793

Mahalakshmi, P., Rajendran, S., Nandhini, G., Joycee, S. C., Vijaya, N., Umasankareswari, T., & Renuga Devi, N. (2020). Inhibition of corrosion of mild steel in sea water by an aqueous extract of turmeric powder. *International Journal of Corrosion and Scale Inhibition*, *9*(2), 706–725. https://doi.org/10.17675/2305-6894-2020-9-2-20

Majd, M. T., Ramezanzadeh, M., Ramezanzadeh, B., & Bahlakeh, G. (2020). Production of an environmentally stable anti-corrosion film based on Esfand seed extract molecules-metal cations: Integrated experimental and computer modeling approaches. In *Journal of Hazardous Materials* (Vol. 382, Issue April). Elsevier B.V. https://doi.org/10.1016/j.jhazmat.2019.121029

Miralrio, A., & Vázquez, A. E. (2020). Plant extracts as green corrosion inhibitors for different metal surfaces and corrosive media: A review. In *Processes* (Vol. 8, Issue 8). MDPI AG. https://doi.org/10.3390/PR8080942

Mobin, M., & Aslam, R. (2018). Experimental and theoretical study on corrosion inhibition performance of environmentally benign non-ionic surfactants for mild steel in 3.5% NaCl solution. *Process Safety and Environmental Protection*, *114*, 279–295. https://doi.org/10.1016/j.psep.2018.01.001

Mohammed, A., & Al-Fakih, A. (2017). *EXPERIMENTAL AND COMPUTATIONAL STUDIES OF FURAN DERIVATIVES IN CORROSION INHIBITION OF MILD STEEL*.

Motamedi, M., Ramezanzadeh, B., & Mahdavian, M. (2018). Corrosion inhibition properties of a green hybrid pigment based on Pr-Urtica Dioica plant extract. *Journal of Industrial and Engineering Chemistry*, *66*, 116–125. https://doi.org/10.1016/j.jiec.2018.05.021

Naghi Tehrani, M. E. H., Ghahremani, P., Ramezanzadeh, M., Bahlakeh, G., & Ramezanzadeh, B. (2021). Theoretical and experimental assessment of a green corrosion inhibitor extracted from Malva sylvestris. *Journal of Environmental Chemical Engineering*, *9*(3). https://doi.org/10.1016/j.jece.2021.105256

Njokua, D. I., Chidieberea, M. A., Oguzieb, K. ., Ogukwea, C. E., & Emeka E. Oguzie*a. (2013). No Title. *Advances in Materials and Corrosion*, *1*, 54–61.

Nwankwo, H. U., Akpan, E. D., Olasunkanmi, L. O., Verma, C., Al-Mohaimeed, A. M., Farraj, D. A. A., & Ebenso, E. E. (2021). N-substituted carbazoles as corrosion inhibitors in microbiologically influenced and

acidic corrosion of mild steel: Gravimetric, electrochemical, surface and computational studies. *Journal of Molecular Structure*, *1223*, 129328. https://doi.org/10.1016/j.molstruc.2020.129328

Oguzie, E. E., Adindu, C. B., Enenebeaku, C. K., Ogukwe, C. E., Chidiebere, M. A., & Oguzie, K. L. (2012). Natural products for materials protection: Mechanism of corrosion inhibition of mild steel by acid extracts of piper guineense. *Journal of Physical Chemistry C*, *116*(25), 13603–13615. https://doi.org/10.1021/jp300791s

Oguzie, E. E., Li, Y., & Wang, F. H. (2007). Corrosion inhibition and adsorption behavior of methionine on mild steel in sulfuric acid and synergistic effect of iodide ion. *Journal of Colloid and Interface Science*, *310*(1), 90–98. https://doi.org/10.1016/j.jcis.2007.01.038

Palaniappan, N., Cole, I., Manickam, S., Thomas, K. R. J., & Santos, D. (2020). *RSC Advances inhibitors for mild steel in NaCl medium †*. *January*. https://doi.org/10.1039/C9RA08971C

Panche, A. N., Diwan, A. D., & Chandra, S. R. (2016). Flavonoids: An overview. *Journal of Nutritional Science*, *5*. https://doi.org/10.1017/jns.2016.41

Papavinasam, S. (2013). Corrosion Control in the Oil and Gas Industry. In *Corrosion Control in the Oil and Gas Industry*. https://doi.org/10.1016/C2011-0-04629-X

Pech-Canul, M. A., & Bartolo-Pérez, P. (2004). Inhibition effects of N-phosphono-methyl-glycine/Zn2+ mixtures on corrosion of steel in neutral chloride solutions. *Surface and Coatings Technology*, *184*(2–3), 133–140. https://doi.org/10.1016/j.surfcoat.2003.11.018

Peng, Y., Hughes, A. E., Deacon, G. B., Junk, P. C., Hinton, B. R. W., Forsyth, M., Mardel, J. I., & Somers, A. E. (2018). A study of rare-earth 3-(4-methylbenzoyl)-propanoate compounds as corrosion inhibitors for AS1020 mild steel in NaCl solutions. *Corrosion Science*, *145*, 199–211. https://doi.org/10.1016/j.corsci.2018.09.022

Rahal, C., Masmoudi, M., Abdelhedi, R., Sabot, R., Jeannin, M., Bouaziz, M., & Refait, P. (2016). AC SC. *JEAC*. https://doi.org/10.1016/j.jelechem.2016.03.010

Ramesh, S., & Rajeswari, S. (2004). *Corrosion inhibition of mild steel in neutral aqueous solution by new triazole derivatives*. *49*, 811–820. https://doi.org/10.1016/j.electacta.2003.09.035

Ramezanzadeh, M., Bahlakeh, G., & Ramezanzadeh, B. (2019a). Study of the synergistic effect of Mangifera indica leaves extract and zinc ions on the mild steel corrosion inhibition in simulated seawater: Computational and electrochemical studies. *Journal of Molecular Liquids*, *292*, 111387. https://doi.org/10.1016/j.molliq.2019.111387

Ramezanzadeh, M., Bahlakeh, G., & Ramezanzadeh, B. (2019b). Study of the synergistic effect of Mangifera indica leaves extract and zinc ions on the mild steel corrosion inhibition in simulated seawater: Computational and electrochemical studies. *Journal of Molecular Liquids*, *292*. https://doi.org/10.1016/j.molliq.2019.111387

Rizvi, M., Gerengi, H., Yildiz, M., Kekecoglu, M., & Pehlivan, M. (2020). *Investigation of ' propolis ' as a green inhibitor of SAE 1010 carbon steel corrosion in 3 . 5 % NaCl environment Investigation of ' propolis ' as a green inhibitor of SAE 1010 carbon steel corrosion in 3 . 5 % NaCl environment*. https://doi.org/10.1021/acs.iecr.0c01239

Sanaei, Z., Ramezanzadeh, M., & Bahlakeh, G. (2018). Journal of Industrial and Engineering Chemistry Use of Rosa canina fruit extract as a green corrosion inhibitor for mild steel in 1 M HCl solution : A complementary experimental , molecular dynamics and quantum mechanics investigation. *Journal of Industrial and Engineering Chemistry*, 1–14. https://doi.org/10.1016/j.jiec.2018.09.013

Sangeetha, M., Rajendran, S., Sathiyabama, J., & Prabhakar, P. (2012). Eco friendly extract of Banana peel as corrosion inhibitor for carbon steel in sea water. *J. Nat. Prod. Plant Resour*, *2*(5), 601–610. http://scholarsresearchlibrary.com/archive.html

Shabani-Nooshabadi, M., & Ghandchi, M. S. (2015). Santolina chamaecyparissus extract as a natural source inhibitor for 304 stainless steel corrosion in 3.5% NaCl. *Journal of Industrial and Engineering Chemistry*, *31*, 231–237. https://doi.org/10.1016/j.jiec.2015.06.028

Singh, A., Lin, Y., Quraishi, M. A., Olasunkanmi, L. O., Fayemi, O. E., Sasikumar, Y., Ramaganthan, B., Bahadur, I., Obot, I. B., Adekunle, A. S., Kabanda, M. M., & Ebenso, E. E. (2015). Porphyrins as corrosion inhibitors for N80 steel in 3.5% NaCl solution: Electrochemical, quantum chemical, QSAR and Monte Carlo simulations studies. *Molecules*, *20*(8), 15122–15146. https://doi.org/10.3390/molecules200815122

Tabatabaei majd, M., Bahlakeh, G., Dehghani, A., Ramezanzadeh, B., & Ramezanzadeh, M. (2019). Combined molecular simulation, DFT computation and electrochemical studies of the mild steel corrosion protection against NaCl solution using aqueous Eucalyptus leaves extract molecules linked with zinc ions. *Journal of Molecular Liquids*, *294*, 111550. https://doi.org/10.1016/j.molliq.2019.111550

Udensi, S. C., Ekpe, O. E., & Nnanna, L. A. (2021). Corrosion inhibition performance of low cost and eco-friendly Treculia africana leaves extract on aluminium alloy AA7075-T7351 in 2.86% NaCl solutions. *Scientific African*, *12*, e00791. https://doi.org/10.1016/j.sciaf.2021.e00791

Verma, C., Ebenso, E. E., & Quraishi, M. A. (2017). Corrosion inhibitors for ferrous and non-ferrous metals and alloys in ionic sodium chloride solutions: A review. *Journal of Molecular Liquids*, *248*, 927–942. https://doi.org/10.1016/j.molliq.2017.10.094

Vijayakumar, S., Krishnakumar, C., Arulmozhi, P., Mahadevan, S., & Parameswari, N. (2018). Biosynthesis, characterization and antimicrobial activities of zinc oxide nanoparticles from leaf extract of Glycosmis pentaphylla (Retz.) DC. *Microbial Pathogenesis*, *116*(December 2017), 44–48. https://doi.org/10.1016/j.micpath.2018.01.003

Wade,Jr., L. G. (2003). (IR) Theory and Interpretation of IR spectra presentation for additional examples of How do we know. *Organic Chemistry*, *5th*, 853–866.

Wang, D., Li, Y., Chen, B., & Zhang, L. (2020). Novel surfactants as green corrosion inhibitors for mild steel in 15% HCl: Experimental and theoretical studies. *Chemical Engineering Journal*, *402*, 126219. https://doi.org/10.1016/j.cej.2020.126219